RATIONALE

Angiogenesis is complex process, involving multiple gene products expressed by different cell types, all contributing to an integrated sequence of events. Consistent with a major role for hypoxia in the overall process, a large number of genes involved in different steps of angiogenesis, including VEGF, are independently responsive to hypoxia. Pathological angiogenesis is a hallmark of cancer and agents that inhibit angiogenesis are attractive therapeutic options [173, 174]. Based on successful preclinical data, several anti-angiogenic agents alone or in combination with conventional therapies are now in clinical trials. Among these agents is 2-methoxyestradiol (2ME2), a natural occurring derivative of estradiol, currently in phase II clinical trials. 2ME2 has been shown to be a well-tolerated small molecule that posses antitumor and antiangiogenic activity in different in vivo models. Although several mechanism have been proposed for 2ME2 activity, its mechanism of action still remains unclear.

Our Hypothesis is that 2ME2 inhibits tumor angiogenesis by targeting the HIF pathway downstream of its effects on the microtubule cytoskeleton. This hypothesis was formulated based on the rationale stated below:

1. Inherent tumor hypoxia is one of the major factors triggering angiogenesis and the cellular response to hypoxia is mediated through the HIF-1 transcription factor. Therefore, we hypothesize that 2ME2 exerts its antiangiogenic properties by inhibiting the α-subunit of the HIF-1 transcription factor in tumor cells.

2. 2ME2 has been reported to inhibit tubulin polymerization *in vitro* upon binding to the colchicine-binding site of the tubulin. Furthermore, the ability of microtubule-targeting agents, especially those binding to the colchicine site (i.e. combretastatins), have been shown to rapidly shut down existing tumor vasculature [2, 175, 176]. Thus, we hypothesized 2ME2 shares with the other colchicine-binding drugs, tubulin as their primary cellular target and that 2ME2's interactions with tubulin in tumor cells mediate the drug's antiangiogenic effects.

In this study we seek to investigate in detail the molecular mechanism by which 2ME2 exerts its antitumor and antiangiogenic properties. More specifically our objectives are: I) Characterize the

molecular mechanism by which 2ME2 inhibits HIF-1 and angiogenesis, II) Investigate whether there is cause-effect relationship between 2ME2's antiangiogenic and anti-tubulin properties.

OBJECTIVES

1. Characterize the molecular mechanism by which 2ME2 inhibits HIF-1 and angiogenesis.

- To investigate the effects of 2ME2 on HIF-1α expression at the transcriptional and post-transcriptional level.
- To investigate the effects of 2ME2 on HIF-1 transcriptional effects
- To investigate the effects of 2ME2 on HIF-1α protein stability and degradation.

2. Investigate whether there is cause-effect relationship between 2ME2's antiangiogenic and anti-tubulin properties

- To investigate whether there is a temporal and spatial relationship between the antitubulin effects of 2ME2 and its effects on the HIF pathway.
- To investigate whether microtubule disruption is required for 2ME2's effects on HIF.
- To investigate whether 2ME2 affects tumor microtubules and HIF-1α *in vivo*, at concentrations that inhibit tumor growth and tumor vascularization.

RESULTS

2ME2 reduces expression of HIF-1α and VEGF in prostate and breast cancer cells.

2ME2 is an effective inhibitor of tumor growth and angiogenesis in numerous *in vivo* models [1, 151, 164]. Although various molecular targets have been proposed for this compound its mechanism of action remains unclear. HIF-1 is a proangiogenic transcription factor stabilized and activated under hypoxia. HIF-1 activates angiogenesis via transcriptional activation of VEGF, among other genes, and consequently is an important tumor survival factor. In this study, we sought to investigate whether regulation of the HIF-1 pathway could contribute to the antiangiogenic effects of 2ME2. We first examined the effects of 2ME2 treatment on HIF-1α protein in the human prostate cancer cells PC-3 (Fig. 11*a*) and in the human breast cancer cells MDA-MB-231 (Fig. 11*b*).

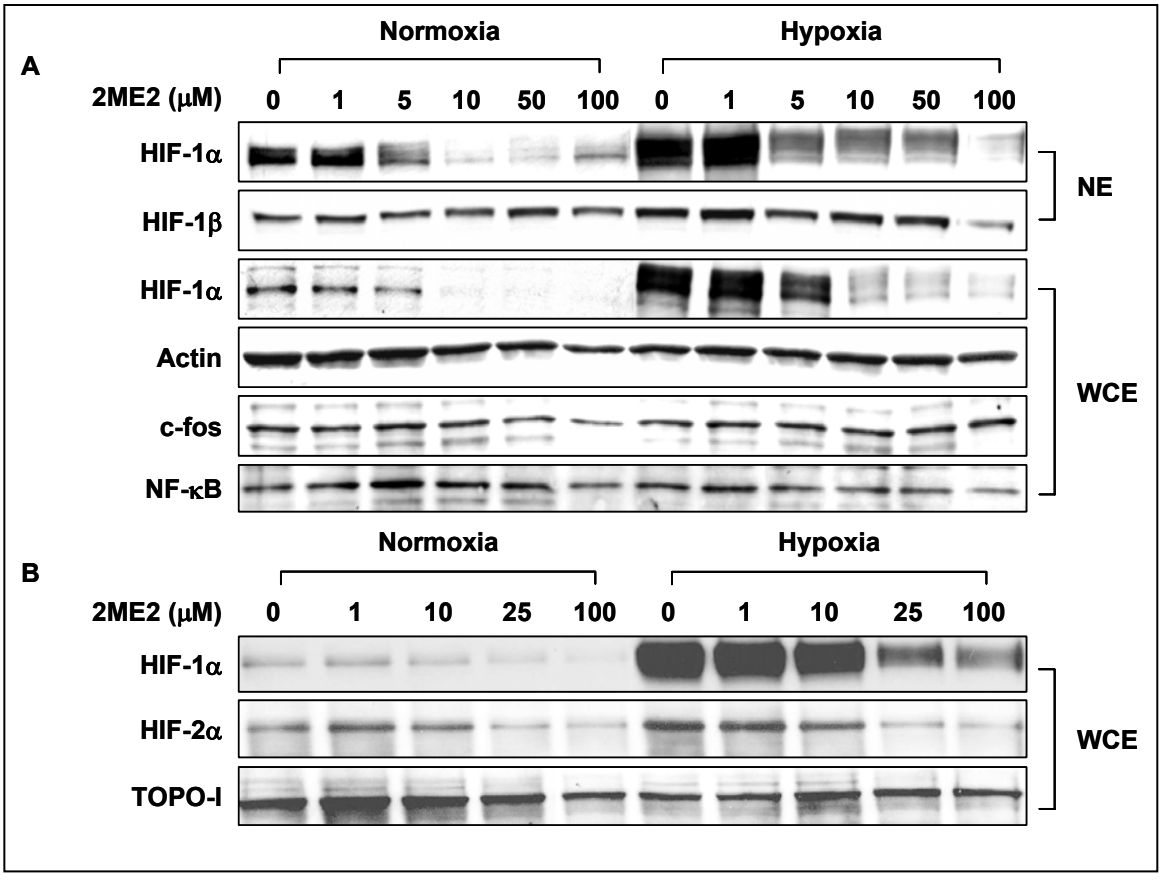

Figure 11. 2ME2 reduces HIF-1a protein levels in a dose-dependent manner. PC3 (A) and MDA-MB-231 (B) cells were treated with increasing concentrations of 2ME2 for 16 hrs and then subjected to hypoxia or remained in normoxia for an additional 6 hrs. Nuclear extracts (NE) or whole cell extracts (WCE) were analyzed by SDS-PAGE and immunoblotted with an antibody against HIF-1α. The blots were stripped and re-probed with HIF-2α, HIF-1β, actin, c-fos, NF-κB.

As shown in Fig. 11, 2ME2 treatment of PC-3 and MDA-MB-231 cells reduced the levels of nuclear and total HIF-1α protein as detected in nuclear (NE) and whole cell extract (WCE) preparations. This inhibition was dose-dependent and seen under both normoxic and hypoxic conditions. HIF-2α, which has been reported to be regulated similarly to HIF-1α [177, 178], is also downregulated by 2ME2 (Fig. 11*b*). Treatment with 2ME2 was specific for the regulated α subunit of HIF-1 and HIF-2 but had no effect on the protein levels of HIF-1β or other transcription factors such as c-fos and NF-κB (Fig. 11a).

To investigate the effects of 2ME2 treatment on HIF-1 transcriptional activity, we measured VEGF protein levels in the conditioned media from 2ME2 treated MDA-MB-231 cells. Consistent with the reduced levels in HIF-1α protein by 2ME2, VEGF levels were also significantly decreased in a dose dependent manner under both normoxic and hypoxic conditions (Fig. 12). Similar results were obtained following treatment of PC-3 cells with 2ME2 (data not shown).

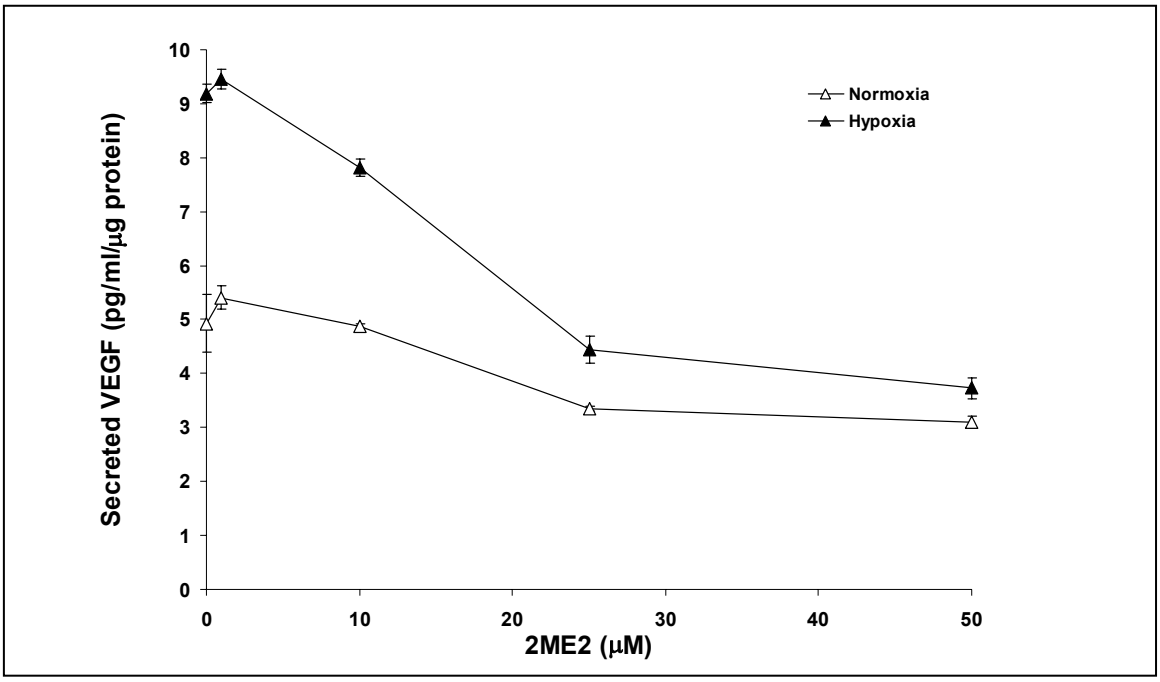

Figure 12. 2ME2 inhibits secreted VEGF. The conditioned media from MDA-MB-231 cells incubated with 2ME2 were analyzed for VEGF. VEGF levels are expressed in pg/ml and were normalized by protein content of each well.

To examine whether the downregulation of VEGF expression after exposure of cells to 2ME2 was the result of a direct effect on HIF-1α, we tested HIF-1 transcriptional activity using a reporter gene assay (Fig. 13).

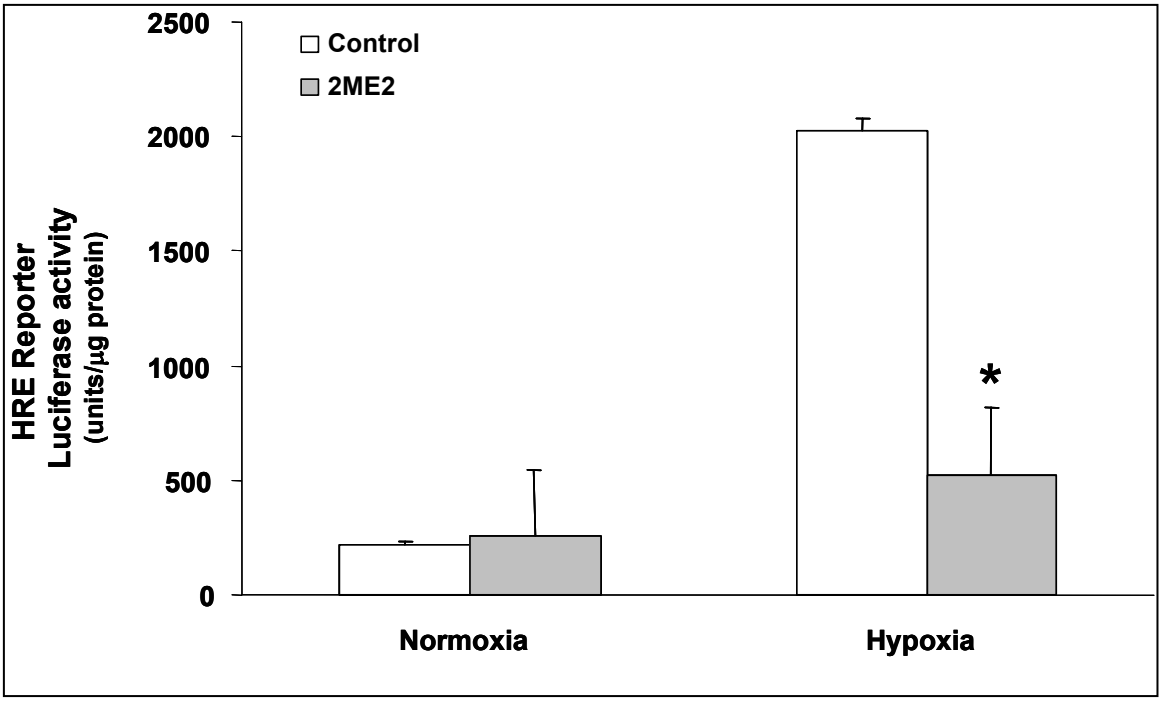

Figure 13. 2ME2 inhibits HIF-1 transcriptional activity. PC3 cells transiently transfected with pBI-GL V6L (6xHREs of VEGF promoter) were treated with vehicle or 100mM of 2ME2 under normoxic and hypoxic conditions. Luciferase reporter activity was measured in the cellular extract 16h later. Luciferase activity represents arbitrary units per mg protein in each assay point. *p<0.05

PC-3 cells were transiently transfected with a construct containing *Luciferase* gene under the control of the hypoxia response elements (HRE) from the *VEGF* promoter [179]. The results show that 2ME2 treatment also blocked the hypoxia-induced transcriptional activity of HIF-1.

To further investigate the effects of 2ME2 treatment on the DNA binding activity of HIF, we performed an electrophoretic mobility shift assay (EMSA) (Fig. 14). Consistent with the gene reporter assay (FIG) HIF DNA binding activity was also attenuated in the 2ME2-treated samples.

Collectively, these results suggest that 2ME2 inhibits the hypoxia-induced DNA binding and transcriptional activity of HIF.

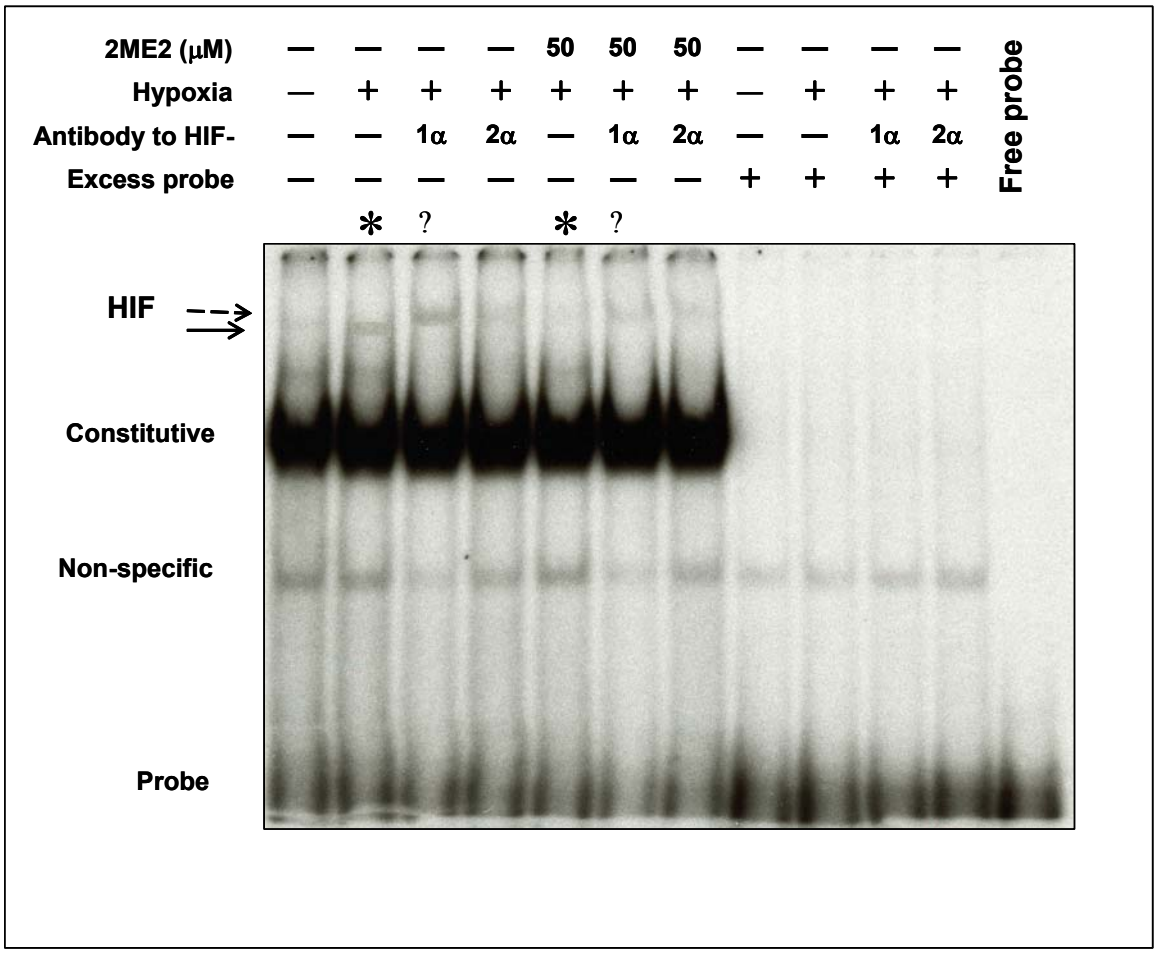

Figure 14. 2ME2 inhibits HIF-1 DNA binding. NE prepared from PC-3 cells untreated or treated with 50 μM 2ME2 under normoxic and hypoxic conditions were subjected to electrophoretic gel mobility shift assay. HIF DNA binding activity is markedly reduced after 2ME2 treatment compared to untreated cells under hypoxia (compare lanes 2 and 5 marked with asterisk). Dashed arrow indicates the supershifting using HIF-1α or HIF-2α specific antibodies. As previously reported, (Kvietikova et al., 1995) in addition to HIF, a constitutive DNA-binding activity also binds the HIF probe in EMSAs. Competition experiments were performed by including a 100-fold excess of unlabeled probe (lanes 8-11) and unbound probe is indicated as free probe (lane 12).

To determine whether downregulation of HIF-1α by 2ME2 occurred at the transcriptional level, we treated MDA-MB-231 cells with 2ME2 and performed Northern blot analysis (Fig. 15). HIF-

1α mRNA levels were not significantly changed by 2ME2 even at very high concentrations (100 μM). Similar results were obtained when we analyzed the expression levels of HIF-1α mRNA with quantitative RT-PCR (data not shown). As expected, hypoxic exposure of the untreated cells resulted in a robust induction (> 20-fold) induction in VEGF mRNA (Fig. 15). 2ME2 treatment significantly decreased VEGF mRNA under normoxia (16-fold decrease) and hypoxia (41-fold decrease). It is of note that 2ME2 inhibited VEGF mRNA (Fig. 15) and secretion (Fig. 12) under normoxic conditions as well. This finding is consistent with the inhibition of HIF-1α protein levels under normoxia. This could be explained by the notion that regulation of VEGF expression in cancer cells with substantial normoxic levels of HIF-1α protein is mediated in part by HIF. In addition, 2ME2 treatment inhibited two other HIF-1 target genes, namely Glut-1 glucose transporter and endothelin-1 (ET-1). This result further confirms that 2ME2 inhibits HIF-1-mediated transcriptional activation of target genes, including VEGF without affecting the transcription of HIF-1α itself.

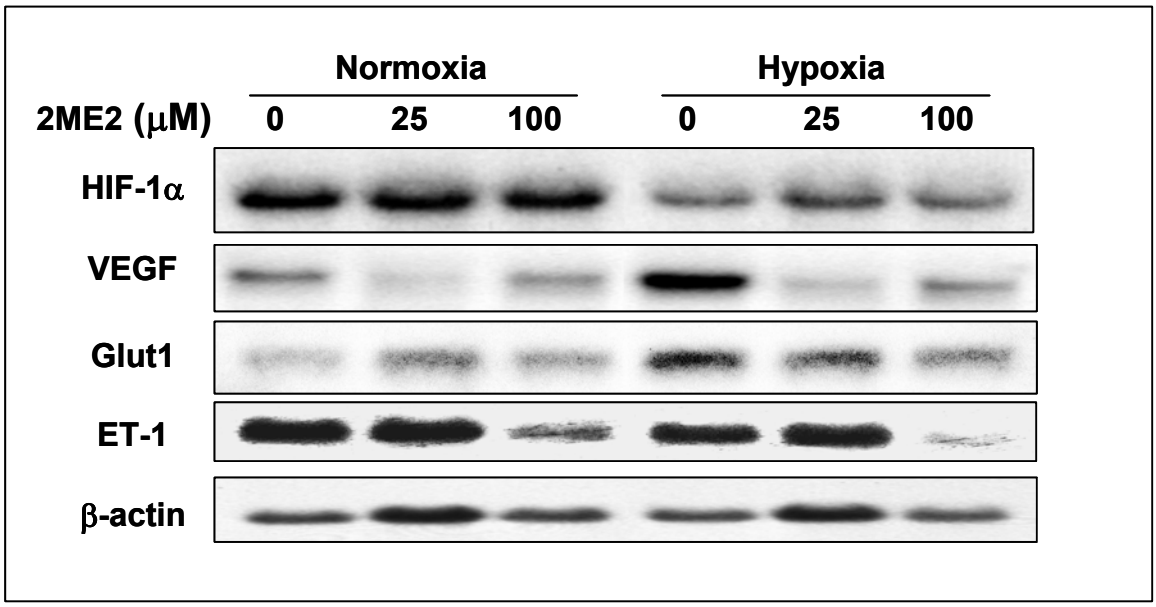

Figure 15. 2ME2 does not inhibit mRNA levels of HIF-1α. Total RNA was prepared from 2ME2 treated MDA-MB-231 under normoxic and hypoxic conditions. Northern blotting was performed with ^{32}P-labeled HIF-1α, $VEGF_{165}$, Glut-1 and ET-1 probes. β-actin is shown as loading control. Quantification of the expression levels of VEGF by densitometry was performed using β-actin.

To obtain a better understanding of the processes involved in HIF-1α inhibition by 2ME2, we studied the effect of 2ME2 on HIF-1α posttranscriptional regulation. We examined 2ME2 effects on HIF-1α protein stability by using the protein translation inhibitor cycloheximide (CHX) (Fig. 16) and a pulse-chase assay (Fig. 17). In the presence of CHX new protein synthesis is inhibited, thus HIF-1α levels would predominantly reflect the degradation process of HIF-1α protein.

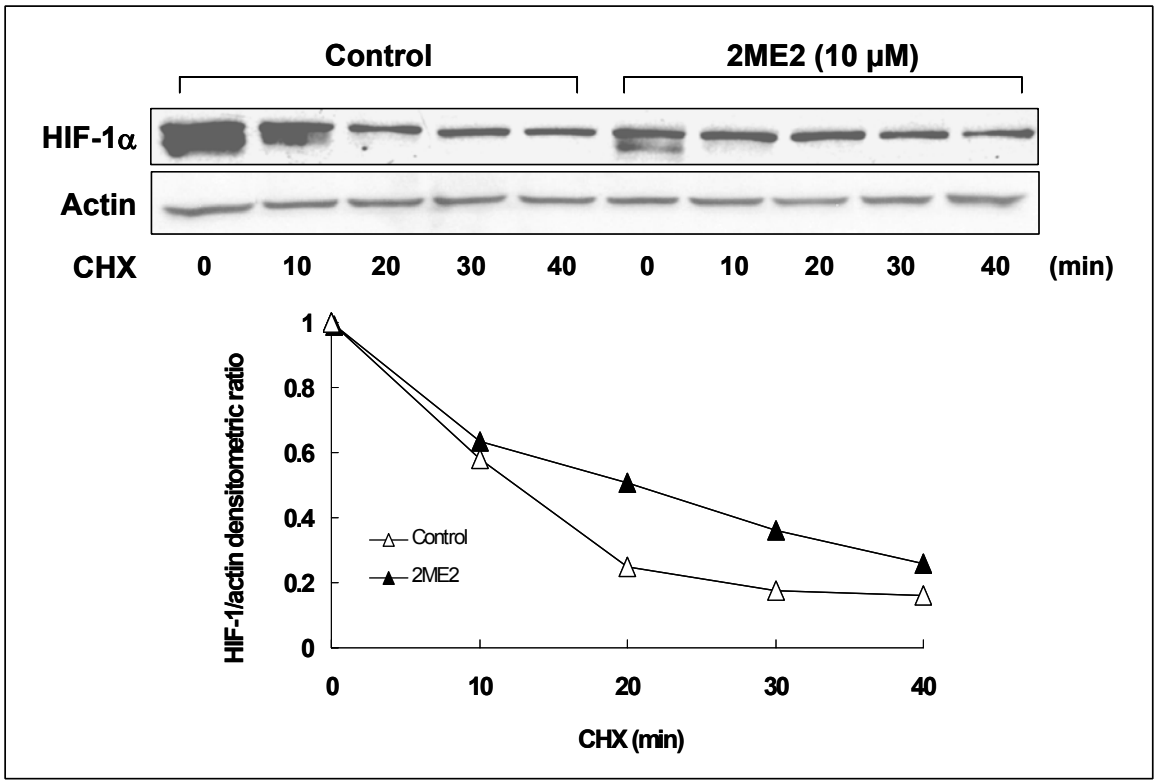

Figure 16. 2ME2 does not accelerate the degradation of HIF-1α protein. *Upper panel:* PC3 were treated overnight with either vehicle (0.01% DMSO) or 10μM of 2ME2 and cycloheximine (CHX) was added at a final concentration of 10μg/ml, for the indicated time. Equal amounts of protein from each sample were resolved by SDS-PAGE and Western blotting was performed with antibodies against HIF-1α or actin. *Lower panel* shows quantification of the HIF-1α signal by densitometry following normalization to actin levels. HIF-1α levels from untreated cells or 2ME2-treated cells are arbitrarily given the value 100%.

Untreated or 2ME2 treated cells were exposed to CHX for various times and HIF-1α protein levels were analyzed by Western blotting. Within 10 min of exposure to CHX (Fig. 16) HIF-1α protein levels from both untreated and treated cells were decreased to about 60%. Although the

intensity of the HIF-1α signal is different at the zero time-point, the degradation rates of HIF-1α protein are similar in the absence or the presence of 2ME2 (Fig. 16).

This was further confirmed when cells were labeled with ^{35}S-methionine and pulse-chased in the presence or absence of 2ME2 (Fig. 17), and HIF-1α protein levels were then analyzed. The half-life of HIF-1α from 2ME2 treated cells was approximately 1.5 h compared to 2.3 h in the untreated cells. Again, as shown in the graph by the slope of the two curves, the rates of HIF-1α protein loss are similar under both conditions. Thus, 2ME2 does not seem to affect directly HIF-1α protein stability, since the rate of decrease of HIF-1α protein from both assays (Fig. 16, 17) is similar in treated and untreated cells.

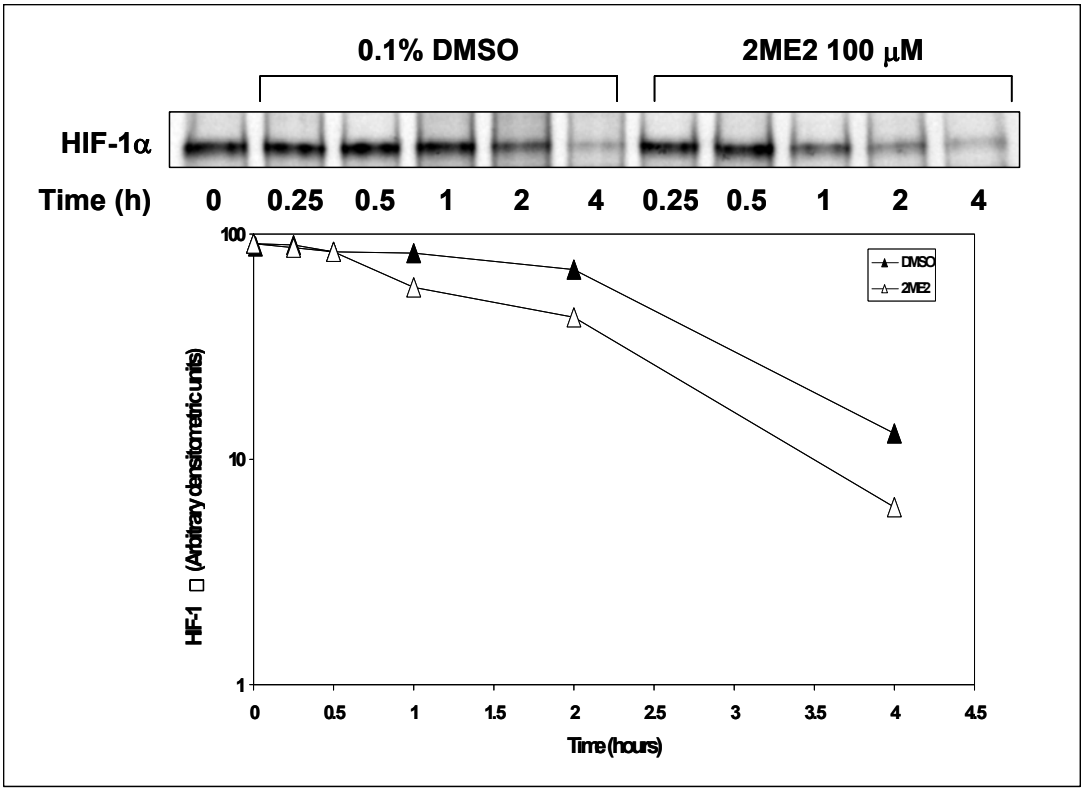

Figure 17. 2ME2 does not affect HIF-1α protein stability. PC3 cells were labeled with ^{35}S-methionine and pulse-chased in complete medium containing either 0.1% DMSO or 100μM of 2ME2 for the indicated time. *Upper panel*: Equal amounts of protein from each cell lysate were subjected to immunoprecipitation with anti-HIF-1α antibody, resolved by SDS-PAGE and subjected to autoradiography. *Lower panel*: Quantification of the autoradiographic HIF-1α signal by densitometry.

Following this observation, we next examined the effect of 2ME2 on HIF-1α protein translation. PC-3 cells were labeled with ^{35}S-methionine in the presence or absence of 2ME2 for the indicated times (min) (Fig. 18).

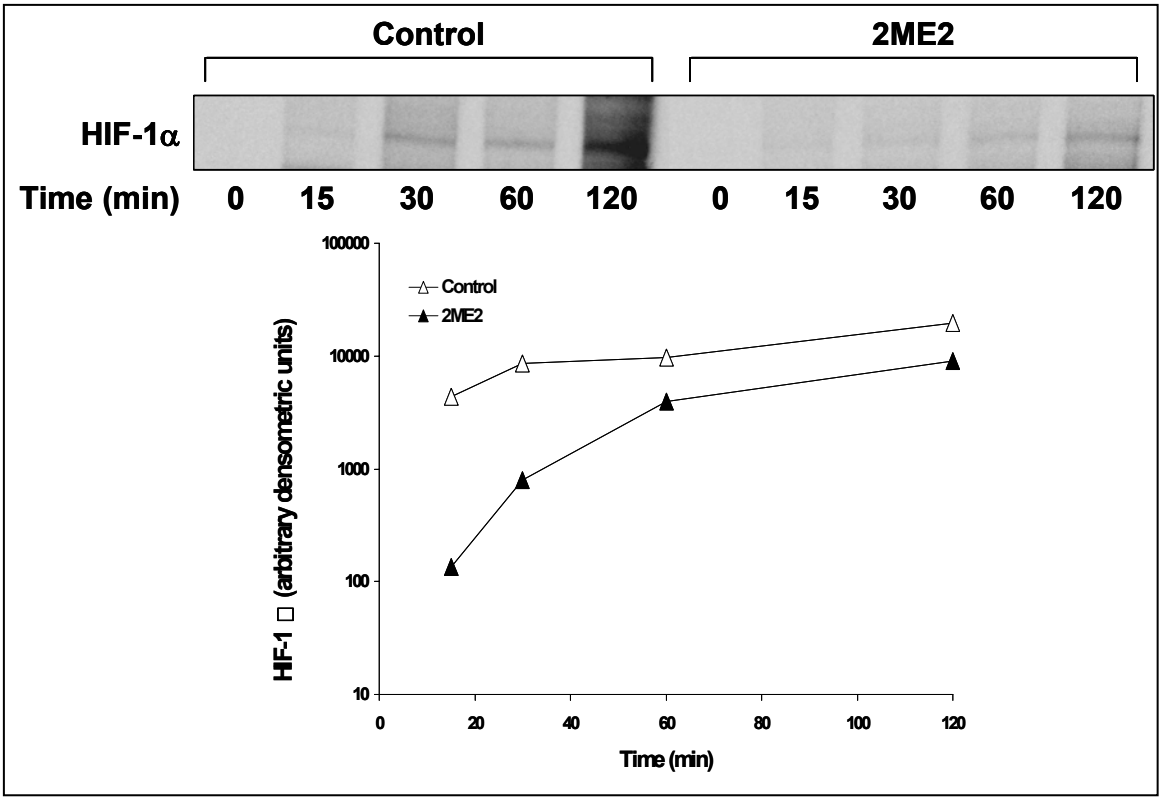

Figure 18. 2ME2 decreases the rate of HIF-1α synthesis. PC3 were pre-treated overnight with either vehicle (0.01% DMSO) or 25μM of 2ME2. The cells were then labeled with 35S-methionine in the presence or absence of 25μM of 2ME2 for the indicated time. *Upper panel*: Equal amounts of protein from each cell lysate were subjected to immunoprecipitation with anti-HIF-1α antibody, resolved by SDS-PAGE and subjected to autoradiography. *Lower panel*: Quantification of the autoradiographic HIF-1α signal by densitometry.

After 15 min of labeling, HIF-1α protein synthesis was at least 10 fold higher in the untreated cells compared with the 2ME2 treated ones (Fig. 18). Together with the results of the protein stability experiments this result suggests that 2ME2 treatment inhibits HIF-1α protein synthesis rather than enhances its degradation. To further exclude the possibility that 2ME2 accelerates HIF-1α ubiquitination and degradation through the proteasome, we performed the experiment shown in Fig. 19. PC-3 cells were treated with 2ME2 in the presence or absence of the

proteasome inhibitor MG-132. In untreated cells, MG-132 resulted as expected in enhanced HIF-1α protein levels and multiple higher ubiquinated HIF-1α protein conjugates (Figure 19, arrows).

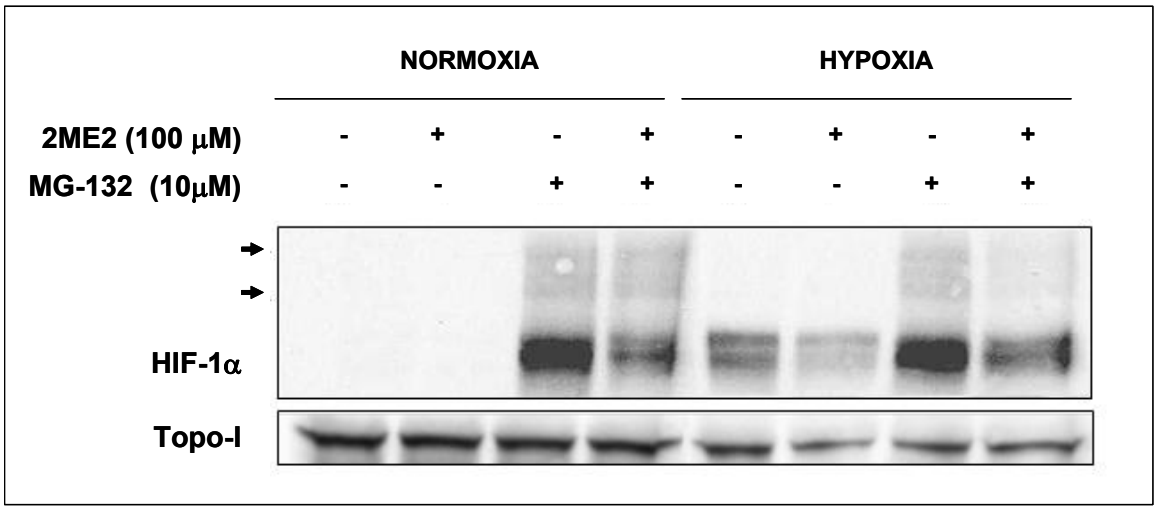

Figure 19. Proteasome inhibitors do not restore the inhibitory effects of 2ME2. PC3 cells were treated with 100μM of 2ME2 in the presence or absence of 10μM of the MG-132 for 4 hrs. Equal amounts of protein from each cell lysate were resolved by SDS-PAGE, transferred and immunoblotted with antibodies against HIF-1a and TOPO-I.

In 2ME2 treated cells however, MG-132, did not restore the inhibitory effect of 2ME2 on HIF-1α protein levels in hypoxia or normoxia, suggesting that 2ME2 does not increase HIF-1α proteasomal-mediated degradation.

To further examine whether 2ME2 effects could be attributed to enhanced HIF-1α ubiquitinylation, we transiently transfected cells with FLAG-tagged HIF-1α and examined the accumulation of the ubiquitinated forms of HIF-1α in the presence or absence of 2ME2. In the presence of 2ME2, there was no change in the amount of ubiquitinated HIF-1α compared to control, indicating that 2ME2 affected HIF-1α prior to the ubiquitination step (Fig. 20).

Although we cannot exclude an indirect effect of 2ME2 in HIF-1α protein degradation through proteasome-independent pathways, our results together with reports on other small molecules

that are known to accelerate HIF-1α ubiquitinylation and proteasomal degradation [180, 181] suggest that 2ME2 reduces HIF-1α protein levels through a translational-dependent pathway rather than affecting HIF-1α protein stability.

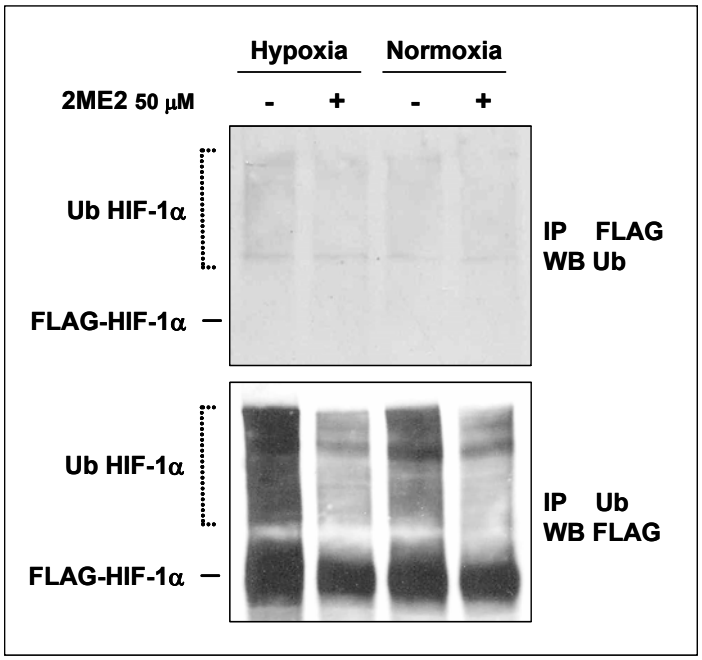

Figure 20. **2ME2 does not enhance HIF-1α ubiquitination.** Cells transiently transfected with p3xFLAG-HIF-1α were treated with vehicle or 50μM 2ME2 under normoxic and hypoxic conditions. The cells were then harvested, whole cell extracts prepared and immunoprecipitation (IP) performed with anti-FLAG antibody. Cell lysates and the immunoprecipitates were resolved on SDS-PAGE and analyzed by Western blot (WB) with ubiquitin (Ub) or FLAG antibodies. The accumulation of poly-ubiquitinated forms of HIF-1α is displayed.

2ME2 depolymerizes microtubules and inhibits nuclear accumulation of HIF-1α

2ME2 has been shown to bind to the colchicine-binding site of tubulin, [166] and to depolymerize microtubules in endothelial [151] as well as in tumor cells [170] resulting in mitotic arrest and cell death. However, there are also reports demonstrating that the antiproliferative activity of 2ME2 may occur independently of the destabilization of microtubules [172] or by actually stabilizing microtubules [182].

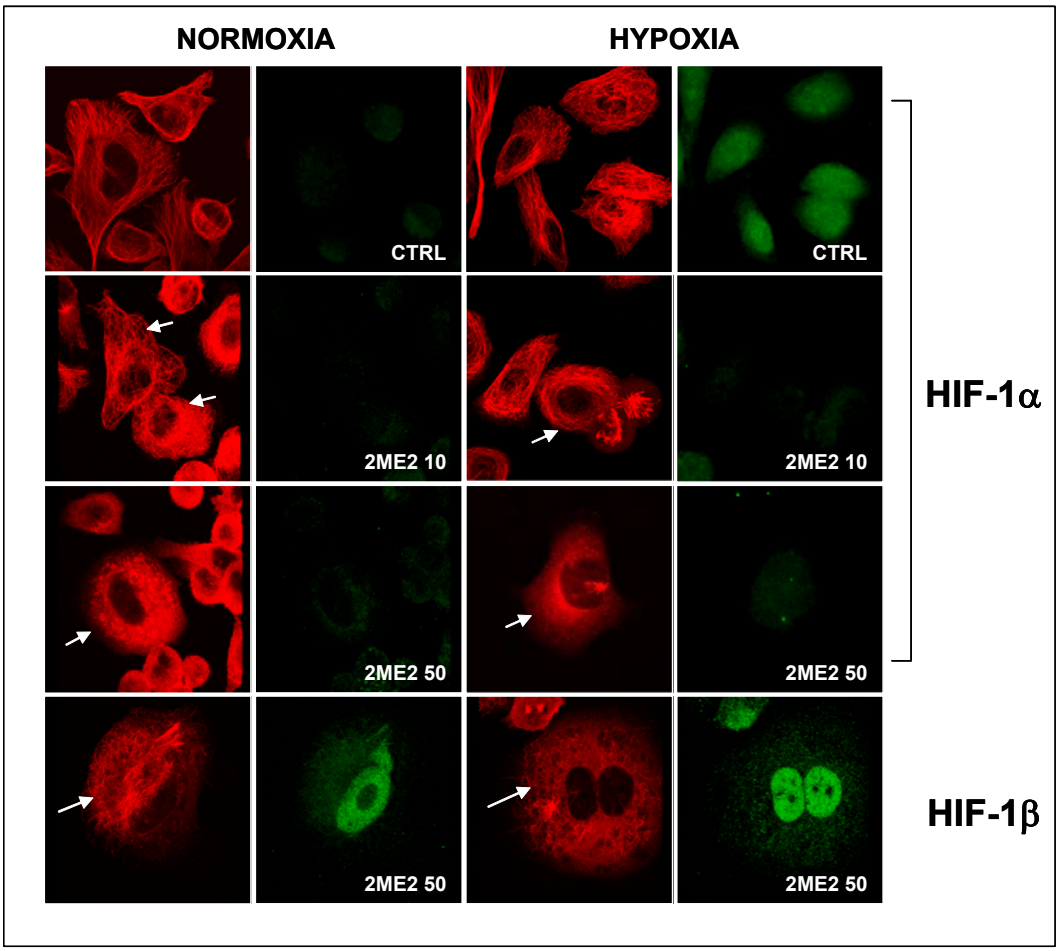

Figure 21. 2ME2 inhibits HIF-1α levels and nuclear accumulation at concentrations that depolymerize MTs. PC3 cells were treated overnight with indicated concentrations of 2ME2 and then subjected to hypoxia. Cells were fixed and processed for double immunofluorescence labeling. HIF-α is shown in green and α-tubulin in red.

Therefore, we sought to investigate whether there is any correlation between the effects of 2ME2 on microtubules and its effects on HIF-1. We assessed this by laser scanning confocal microscopy (LSCM) in PC3 cells treated with 2ME2 (Fig. 21). The cells were double-labeled with antibodies against α-tubulin (red) and HIF-1α (green) (Fig. 21).

We observed a dose-dependent depolymerization of microtubules in the 2ME2 treated cells (solid arrows) compared to the fine and intricate microtubule network observed in untreated control cells. No significant changes in the microtubule network were observed in untreated cells after hypoxia. On the other hand, while HIF-1α was barely detectable under normoxic conditions, it predominantly accumulated in the nucleus after exposure to hypoxia (Fig. 21, green staining). 2ME2 treatment significantly reduced the hypoxia-induced nuclear accumulation of HIF-1α. To examine whether these effects were specific for the regulated subunit of HIF-1, HIF-1α, we also tested the effects of 2ME2 on HIF-1β. As seen at the bottom panel of Fig.21, 2ME2 treatment had no effect on either HIF-1β (green) levels or on HIF-1β subcellular localization. In untreated cells, HIF-1β was localized predominantly in the nucleus and it was not further accumulated after hypoxia (data not shown).

To determine if the inhibition of HIF-1α was a general property of MT-targeting agents or whether it was specific to 2ME2, we tested other MT-disrupting agents that either destabilize (vincristine) or stabilize (Taxol) MTs (Fig. 22). Treatment of PC-3 cells with Taxol stabilized MTs resulting in distinct microtubules bundles (dashed arrows), while vincristine completely depolymerized microtubules (solid arrows) (Fig. 22). Similarly to 2ME2, both Taxol and vincristine blocked the hypoxia-induced nuclear accumulation of HIF-1α (Fig. 22) while they had no effect on HIF-1β (Fig. 3*b* and vincristine data not shown).

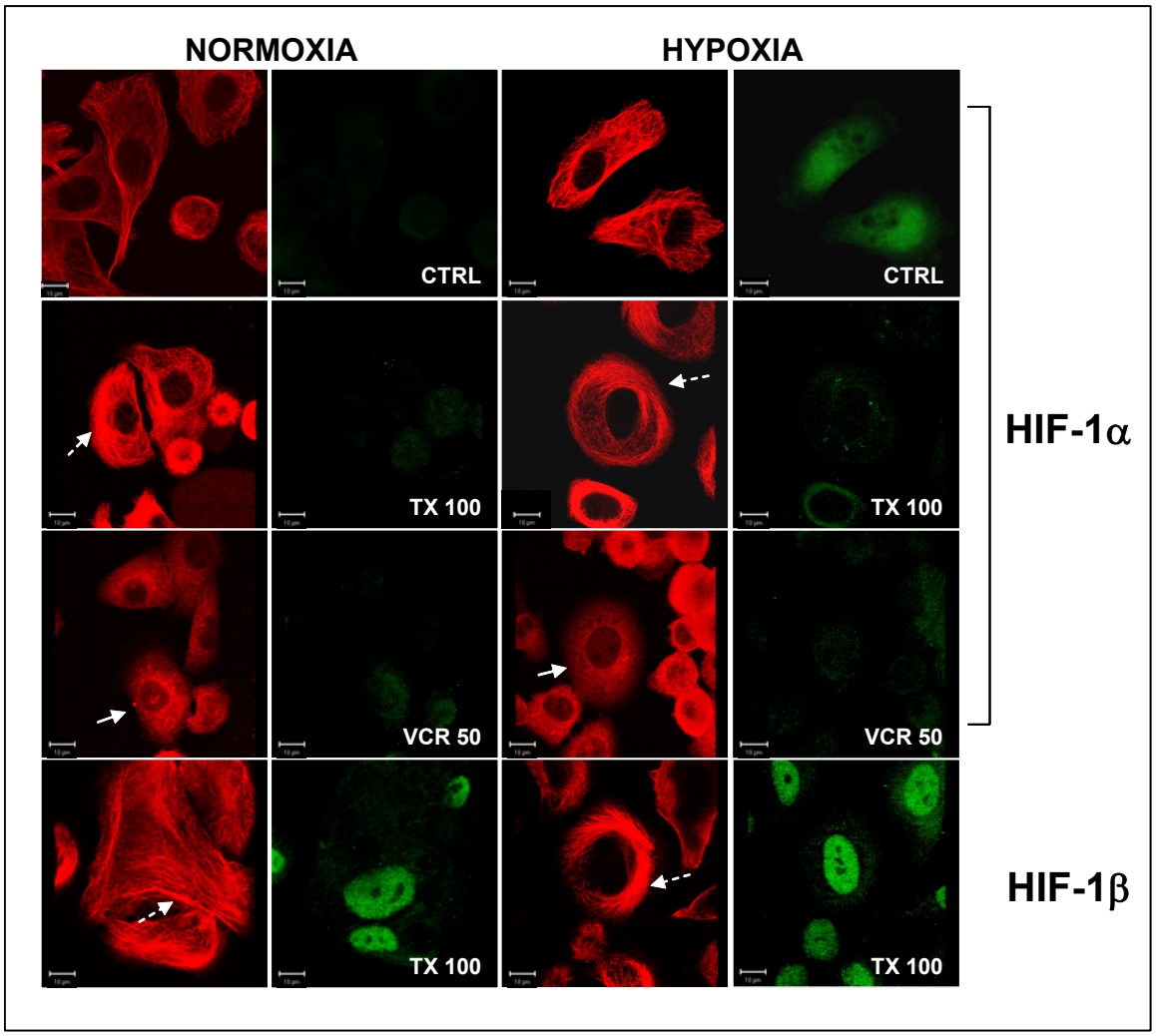

Figure 22. Microtubule-targeting drugs decrease HIF-1α levels and nuclear accumulation at concentrations that disrupt cellular MTs. PC3 cells were treated overnight with Taxol and Vincristine and then subjected to hypoxia. Cells were fixed and processed for double immunofluorescence labeling. HIF-α is shown in green and α-tubulin in red.

To confirm the data obtained by immunofluorescence and LSCM, we analyzed HIF-1α protein levels and HIF-1 transcriptional activity in cells treated with Taxol and vincristine, utilizing 2ME2 as a positive control. Consistent with what was observed with 2ME2 and with their effects on microtubules (Fig 23), Taxol and vincristine also reduced HIF-1α protein levels in a dose-dependent manner (Fig 23, *upper panel*) and inhibited HIF-1 transcriptional activity (Fig. 23, lower panel).

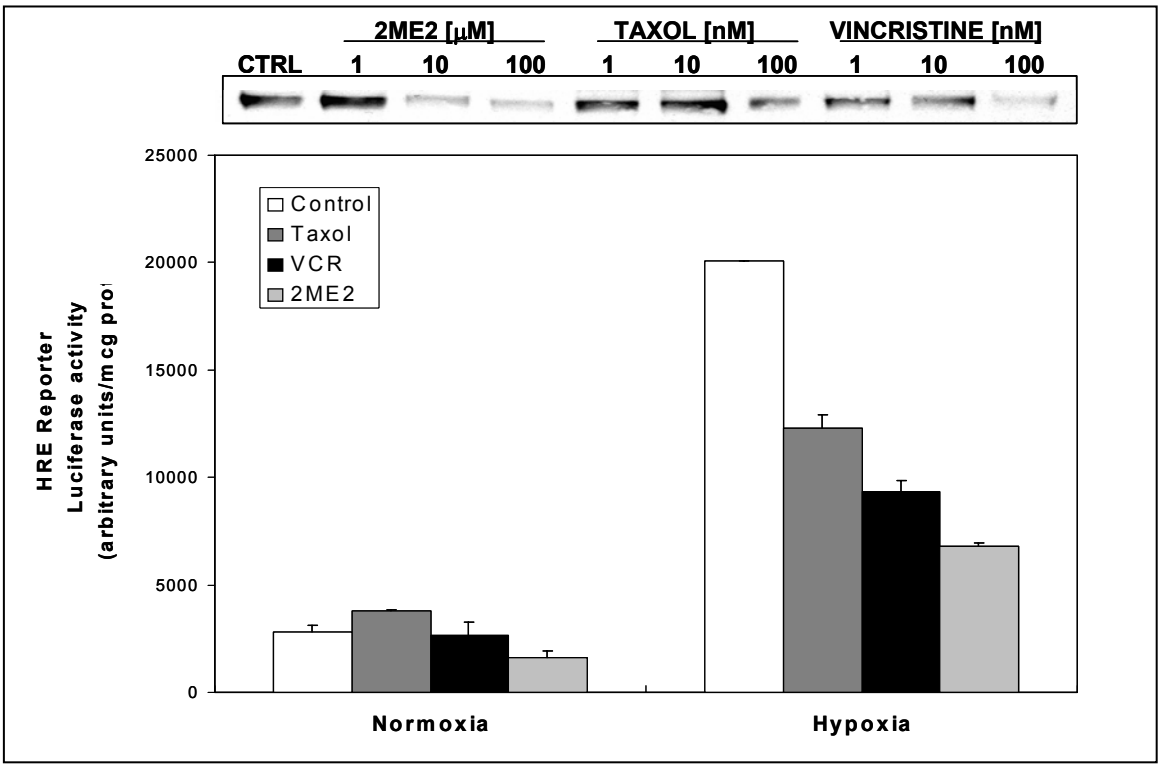

Figure 23. 2ME2 decreases the rate of HIF-1α synthesis. PC3 transiently transfected with pBI-GL V6L were treated with vehicle, 2ME2, Taxol or Vincristine under normoxic or hypoxic conditions. The cells were then harvested and analyzed for luciferase activity. The upper panel shows a Western blot developed with a HIF- 1α antibody of nuclear extracts (NE) of cells treated with the indicated drug concentrations under hypoxia.

Since MT-targeting drugs are known to cause mitotic arrest, we wanted to exclude the possibility that the effects of 2ME2, Taxol and vincristine on HIF-1α were non-specific and reflected rather a "side effect" of mitotic arrest. Thus, we treated MDA-MB231 cells with monastrol (Fig. 24), a compound known to induce mitotic arrest by inhibiting the mitotic kinesin Eg5 but has no effect on the organization or function of the microtubule cytoskeleton [183]. As clearly shown in Fig. 24, monastrol has no effect on HIF-1α protein levels (upper panel) even at concentrations that induce a profound mitotic arrest (lower panel). Consistent with previously published reports on monastrol, [184] and unlike MT-targeting drugs, we also see no effect on interphase microtubules even at concentrations that monoastral spindles are observed (Fig. 24, lower panel). Collectively, these results suggest that the strong link between disruption of the microtubule cytoskeleton and inhibition of HIF-1α function is independent of mitotic arrest.

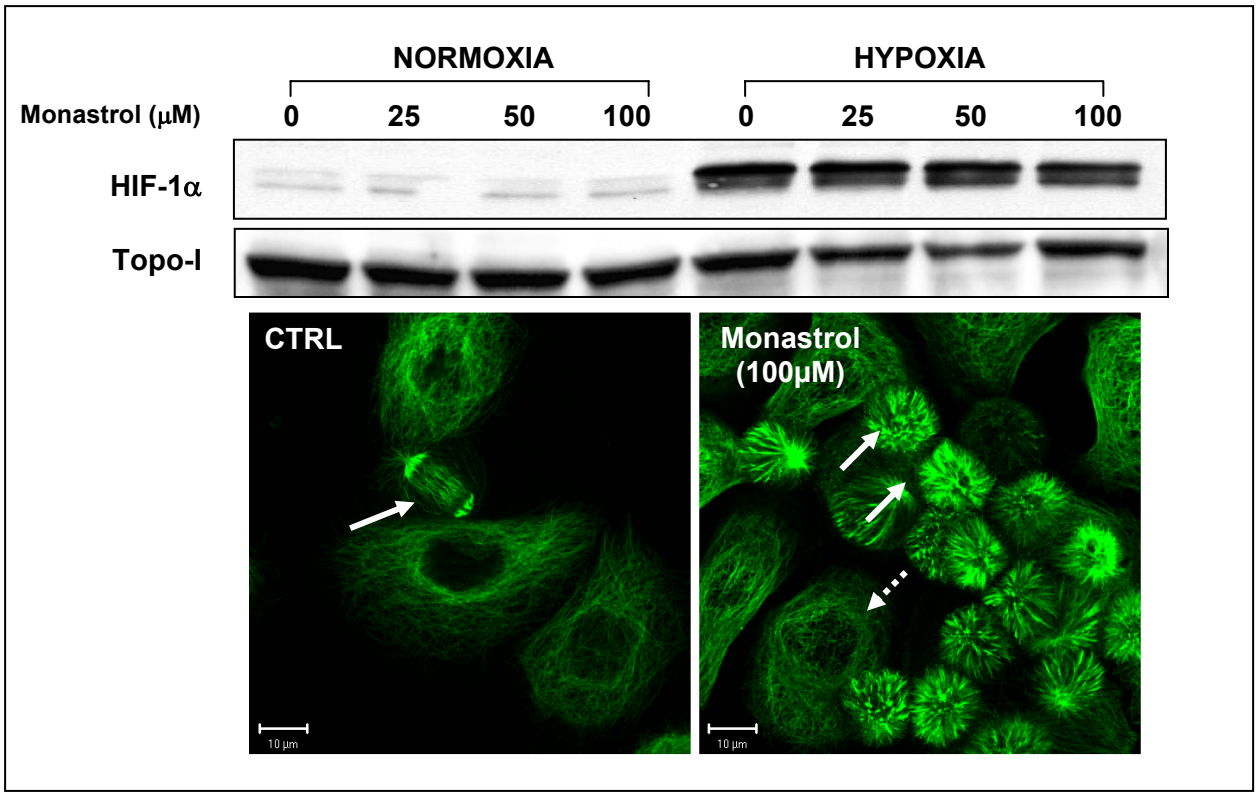

Figure 24. 2ME2 does effects on HIF-1α are not due to mitotic arrest. PC3 cells were cells were treated with increasing concentrations of Monastrol for 16 hrs and then subjected to hypoxia or remained in normoxia for an additional 6 hrs. *Upper panel*: Cell extracts were analyzed by SDS-PAGE and immunoblotted with an antibody against HIF-1α. *Lower panel*: Cells were fixed and processed for single immunofluorescence labeling. Microtubules are shown in green. Solid arrows depict mitotic cells and dotted arrows interphase cells. Notice the difference between a cell normally undergoing mitosis in control cells (telophase) versus the abnormal monoastral mitotic spindles induced by monastrol

Disruption of the MT-cytoskeleton is required for HIF-1α inhibition.

The data with these three different classes of MT-targeting drugs indicate that there is good correlation between the disruption of the MT-cytoskeleton and the inhibition of HIF-1α. However, the question remains on whether the effects of the MT-targeting drugs on HIF-1α are independent from their effects on the MT-cytoskeleton.

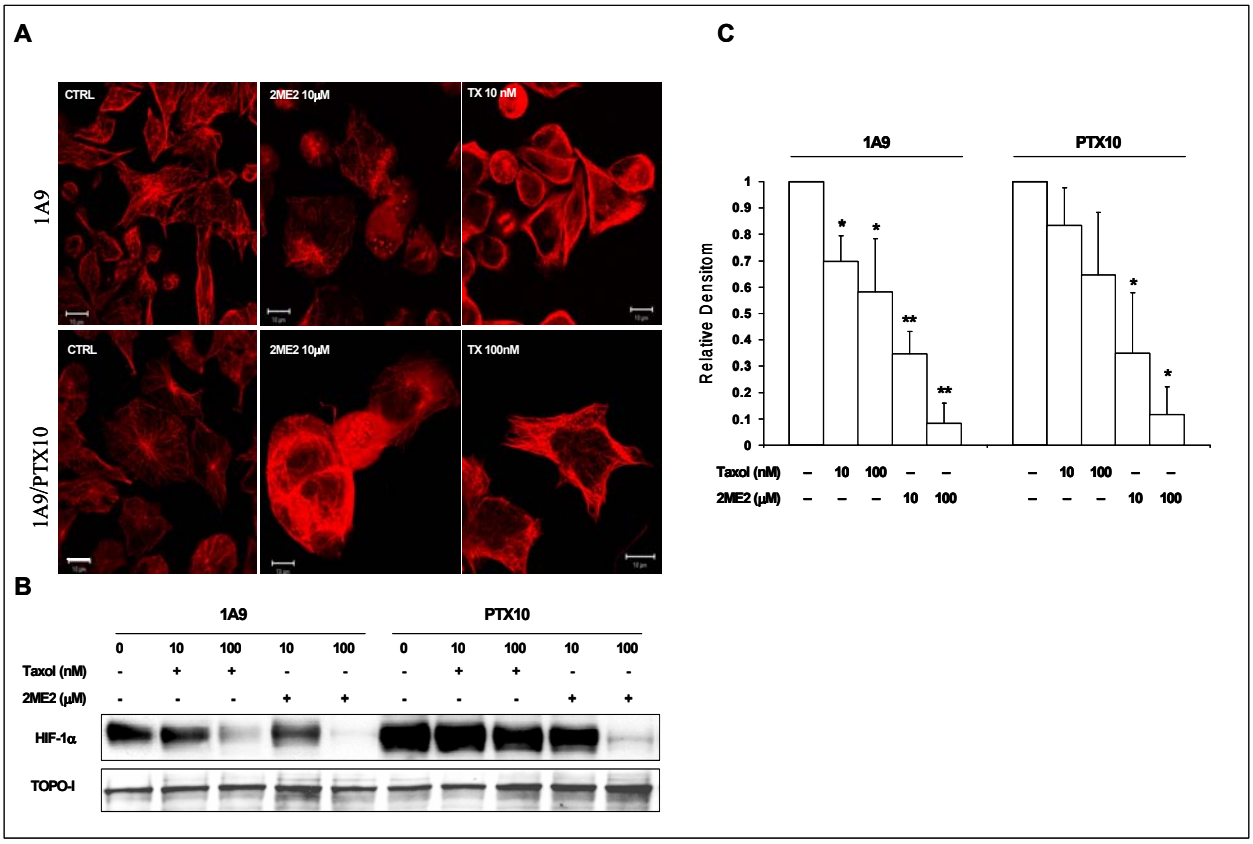

Figure 25. Drug-tubulin interaction is required for inhibition of HIF-1α protein expression. 1A9 and PTX10 cells were plated in duplicate, subjected to the indicated treatments overnight followed by hypoxia for an additional 6 hrs, and processed for confocal microscopy (**a**) and Western blotting (**b**). ***a*** Cells were prepared for immunofluorescence staining with an anti-α-tubulin antibody followed by a secondary Alexa 568 antibody. Scale bar, 10 μm. ***b***, Equal amounts of protein from each cell lysate (NE) were resolved by SDS-PAGE, transferred and immunoblotted with antibodies against HIF-1α and TOPO-I. ***c.*** Densitometric quantification and statistical analysis of three independent repetitions of the experiment described above. HIF-1α/TOPO-I levels from untreated cells of each experiment were given the value of 1 (100%). Relative densitometry represents arbitrary units of the mean of the 3 repetitions included in this analysis. *Columns*, means; *bars*, SD; n = 3; *, $P < 0.05$; ** $P < 0.01$**.**

We addressed this question through a genetic approach employing the 1A9 human ovarian carcinoma cells and its Taxol-resistant clone, 1A9/PTX10 [185]. The 1A9/PTX10 cells are 30-fold resistant to Taxol due to an acquired β-tubulin mutation at the Taxol binding site, while they retain sensitivity to all MT-depolymerizing agents [185] including 2ME2. To assess whether drug induced effects on microtubules is necessary for inhibition of HIF-1α, we treated the parental 1A9 and the Taxol-resistant 1A9/PTX10 cells with Taxol and 2ME2 and processed them for LSCM and Western blot analysis (Fig. 25). As expected, Taxol had no effect on the microtubule network in 1A9/PTX10 cells even at 100nM, whereas as little as 10nM of Taxol was sufficient to bundle microtubules in the 1A9 parental cells (Fig. 25a). In addition, Taxol inhibited HIF-1α protein levels in the parental 1A9 cells only, while it had almost no effect on HIF-1α levels in 1A9/PTX10 cells. In contrast, 2ME2 depolymerized MTs and reduced HIF-1α protein levels in both 1A9 and 1A9/PTX10 cells (Fig. 25*a* and 25*b*). Statistical analysis of three independent experiments (Fig. 25c) shows that the ability of Taxol and 2ME2 to inhibit HIF-1α levels correlates very well with their ability to affect cellular microtubules. These data extend our previous observations and further suggest that disruption of the normal of the MT-cytoskeleton is required for HIF-1α inhibition by MT-targeting drugs.

2ME2 inhibits angiogenesis at concentrations that disrupt microtubules *in vivo*.

The concentrations of 2ME2 required to observe the effects on microtubules *in vitro* are much higher than those achievable *in vivo*. We employed a mouse orthotopic breast tumor model to determine whether 2ME2 disrupts microtubules at the same doses at which it exhibits antitumor activity *in vivo,* and to see if this also results in a decrease in the tumor microvascular density. Animals were treated with 2ME2 or cyclophosphamide as a non-MT-targeting chemotherapy drug. At the end of treatment tumors were excised and processed to assess several different parameters such as tumor volume, vascularization, and integrity of the MT-cytoskeleton.

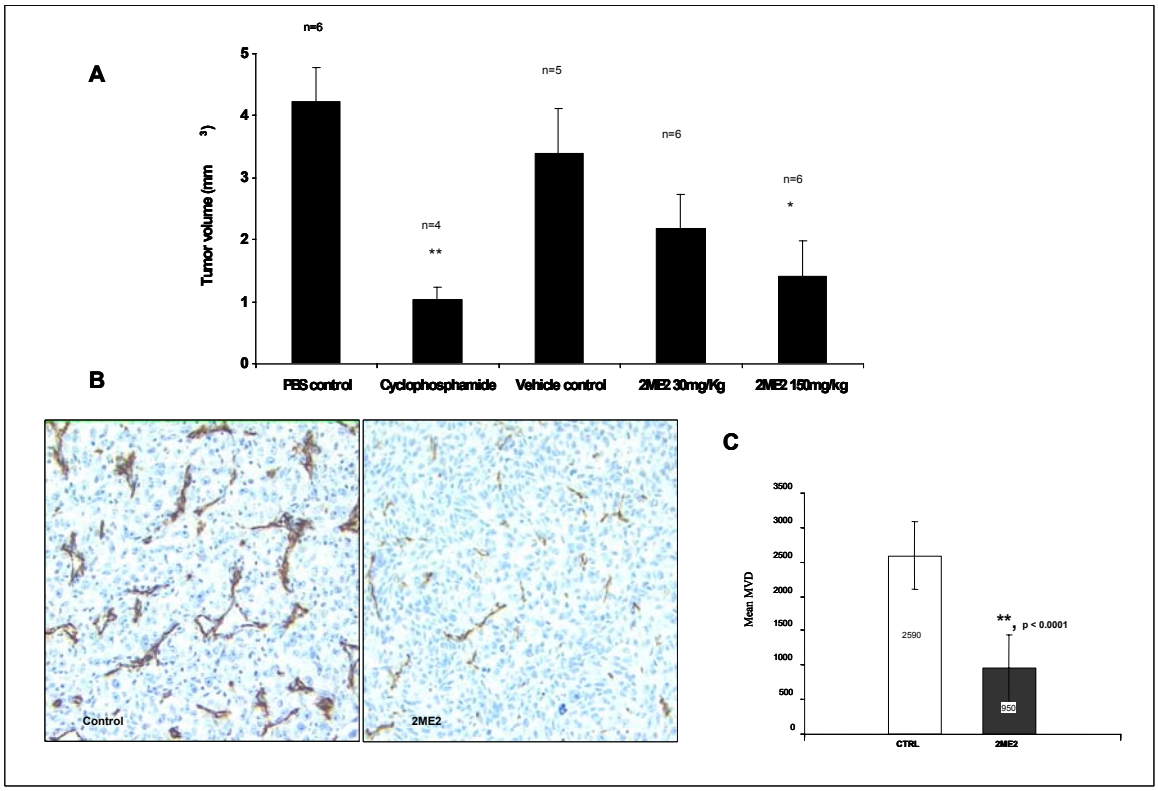

Figure 26. 2ME2 inhibits tumor growth *in* vivo. A breast cancer orthotopic model was established using human MDA-MB-231 cells ($2x10^6$) implanted into the mammary fat pad of female BALB/c nu/nu mice. Animals were treated with the indicated drugs as described in Materials and Methods, sacrificed after 33 days of treatment and their tumors were processed for tumor volume measurements ***a***, Tumor volume measurements were calculated using the formula $width^2$ x length x 0.52. Mean ± SE of representative experiments is shown. *, $P < 0.05$ compared to 1% HPMC vehicle control; **, $P < 0.01$ compared to PBS control ***b*,** Microvessel density (MVD) was determined by CD31 immunostaining in 10 paraffin-embedded tumor sections from each animal per cohort. 20x magnification is shown; 2ME2 150mg/kg. ***c*,**: Statistical analysis of MVD from all control and 2ME2 (150 mg/kg) treated animals. Columns represent mean MVD and bars represent +/- SEM.

As seen in Fig. 26a, a dose-dependent reduction of tumor volume was observed with 2ME2 treatment, and at 150 mg/kg there is a significant reduction in tumor volume when compared to the vehicle treated control animals (Fig.26*a*). In addition, time-dependent tumor growth inhibition was also observed. To study the effects of 2ME2 on tumor vascularization we performed immunohistochemical staining for CD31 in untreated and 2ME2 treated animals and representative images are shown in Fig. 26b. A clear reduction of CD31 staining is seen in the treated animals compared to controls (Fig. 26b). Statistical analysis of microvessel density

(MVD) from CD31 immunostained tumors was performed by analyzing at least 10 sections from each mouse per cohort. This analysis revealed a significant decrease ($p<0.0001$) in MVD in animals treated with 2ME2 compared to controls (Fig. 26c).

Then we sought to investigate whether the *in vivo* effects of 2ME2 on MVD correlated with its antitubulin effects, as we have seen in our experiments with cultured cells. The *in vivo* effect of 2ME2 on MTs was evaluated by two different assays. First, we developed a highly sensitive method to allow qualitative assessment of the MT-cytoskeleton integrity *in vivo*, using LSCM of tumor sections stained with an antibody against tubulin as described under "Materials and Methods". As shown in Fig. 27 the tumor cells from vehicle or cyclophosphamide-treated mice (animal #17, and #11, respectively) possess a fine, intricate and well-organized microtubule network (solid arrows). In contrast, the tumor cells from the animals treated with 150 mg/kg 2ME2 (animal #19 and #21a, b) possess either completely depolymerized MTs (dashed arrows) or multiple mitotic asters (dotted arrows), which indicate aberrant mitotic arrest. The latter is more evident in the lower magnification field shown for animal #21 (21b) where almost every cell displayed has aberrant mitotic spindles. The tumor cells from animals treated with 30 mg/kg 2ME2 (animal #29) also have depolymerized MTs (dashed arrows) and multiple aberrant mitotic asters (dotted arrows). This is the first report of a qualitative assessment of microtubules *in vivo*.

A section of each tumor excised was processed for Western blot for tubulin analysis, in order to assess quantitatively the relative levels of polymerized and soluble tubulin following 2ME2 treatment (Fig. 28). In this experiment we adapted this technique previously developed to assess the effects of MT-targeting drugs on cultured cells [185]. From each tumor the lanes labeled "P" contain the polymerized form of tubulin (MTs) and those labeled "S" the soluble form (α/β tubulin dimers). Treatment with 2ME2 depolymerized MTs in a dose-dependent manner as evidenced by the decrease from 70% of polymerized tubulin in the vehicle-treated animal to 3%-9% observed in the animals treated with 2ME2. Thus, we have demonstrated by two independent assays that 2ME2 depolymerizes MTs *in vivo* (Fig. 27, 28) at concentrations that inhibit growth and vascularization of tumors (Fig. 27).

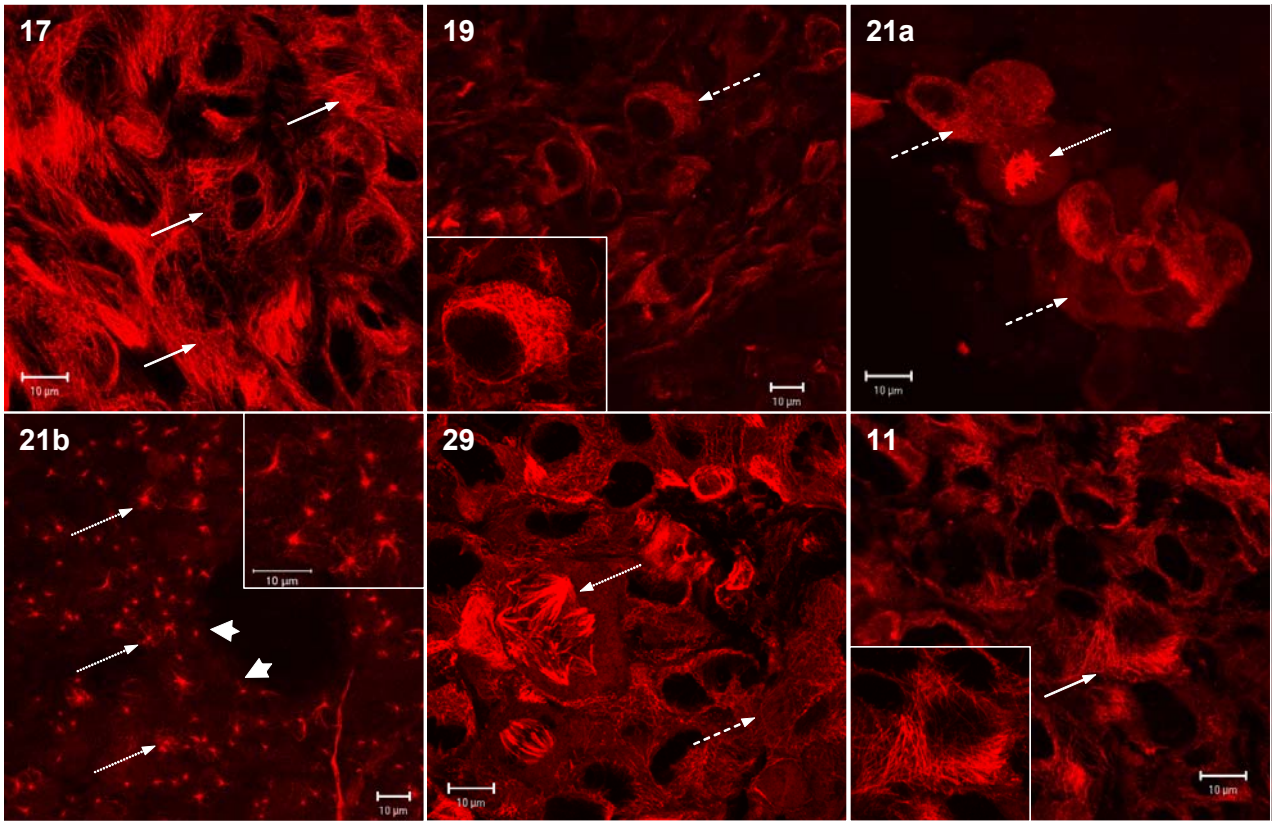

Figure 27. 2ME2 inhibits angiogenesis at concentrations that depolymerized microtubules *in vivo*. Animals treated with the indicated drugs above were sacrificed 33 days later of treatment, and their tumors were processed for tubulin immunofluorescence staining with an anti-α-tubulin antibody (red staining) in 50 µm thick tumor sections from treated and untreated animals as indicated. Sections were analyzed by confocal microscopy. Representative treated animals from each treatment cohort are shown as follows: animal **#17**, vehicle treated animal; **#19**, and **#21**, 2ME2 treated animals at 150 mg/kg; **#29**, 2ME2 treated animal at 30 mg/kg; **#11**, cyclophosphamide treated animal. Solid arrows depict the fine and intricate microtubule network from untreated animal **#17** or from cyclophosphamide treated animal **#11** (inset shows higher magnification of one cell from the entire field). Dashed arrows depict cells with depolymerized microtubules from 2ME2 (150 mg/kg) treated animals **#19**, and **#21**. Inset in **#19**, shows a higher magnification of a cell with profound MT-depolymerization. Dotted arrow in **#21a,** depicts a cells with abnormal mitotic asters as a result of 2ME2 treatment. Dotted arrows in **#21b** (lower magnification) depict cells with aberrant mitotic spindles abnormally arrested in mitosis after 2ME2 treatment. Inset in **#21b** shows a higher magnification of cells with aberrant mitotic spindles. Thick arrowheads point at aberrant mitotic cells lining the vessel. Dashed arrow in **#29**, depicts cells with depolymerized MTs and dotted arrow cells with aberrant mitosis after treatment with 30 mg/kg 2ME2. Scale bars, 10 µm.

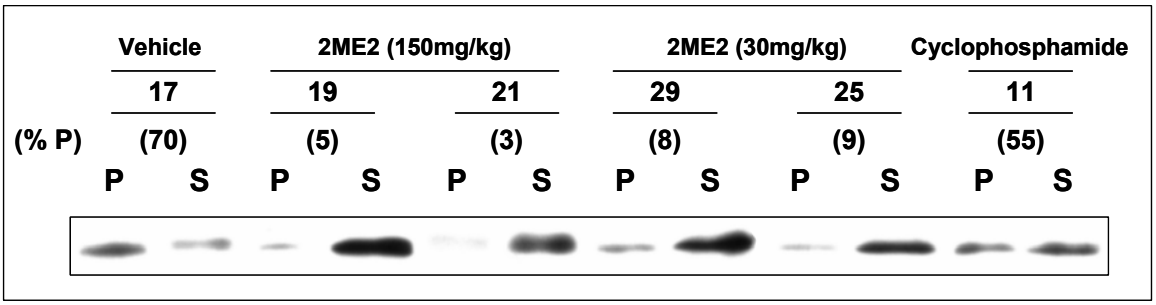

Figure 28. 2ME2 depolymerizes microtubules *in vivo*. The relative levels of polymerized and soluble tubulin from each treated animal were analyzed in excised tumors from treated or untreated mice. After centrifugation, the pellet (P) (polymerized tubulin) and supernatant (S) (soluble tubulin dimers) fractions from each reaction were prepared for Western Blotting with anti-α-tubulin. The percentage of polymerized (% P) tubulin from the tumor of each animal was determined by dividing the densitometry value of polymerized tubulin by the total tubulin content.

Then we sought to investigate whether 2ME2 also inhibited HIF-1α *in vivo* at the doses that effectively inhibited tumor growth, tumor angiogenesis and depolymerized tumor microtubules. We analyzed tumor sections from untreated animals or animals treated with 150mg/kg 2ME2 by immunohistochemistry. As shown in Fig. 29, 2ME2 treatment not only decreased HIF-1α protein expression, but also impaired the nuclear accumulation of HIF-1α compare the sharp and intense nuclear HIF-1α staining in the control (Fig. 29 solid arrows and inset) with the diffuse cytoplasmic HIF-1α staining in the 2ME2 treated samples (Fig. 29, dashed arrows and inset).

Careful examination of the in vivo MT staining after 2ME2 treatment suggested that 2ME2 may also have an effect on endothelial cell tubulin, as depicted by the aberrant mitoses seen in cells that line the vessel in animal #21b (Fig. 5c, thick arrowheads). This observation prompted us to investigate the effects of 2ME2 on endothelial cells *in vitro* and *in vivo*. As shown in Fig. 30 and similarly to cancer cells (Fig. 11), 2ME2 treatment resulted in a dose-dependent inhibition of HIF-2α protein in human umbilical vein endothelial cells (HUVEC) (Fig. 30a, upper panel), which correlated with extensive microtubule depolymerization (Fig.30a, lower panel). Decreased DNA binding activity of HIF measured by EMSA was observed in 2ME2 treated HUVEC cells compared to control untreated cells (data not shown).

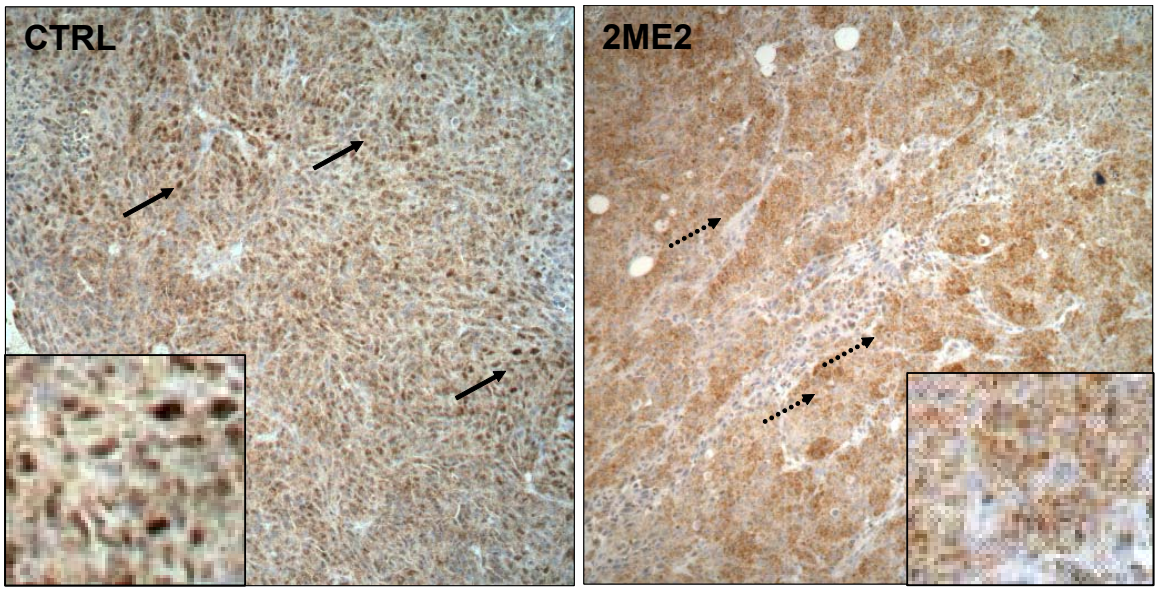

Figure 29. 2ME2 inhibits HIF-1α protein expression *in vivo*. Tumor sections from untreated (CTRL) or 2ME2 (150 mg/kg) treated animals were immunohistochemically stained with HIF-1α antibody. Solid arrows: nuclear staining in control tumors; Dashed arrows: diffused cytoplasmic staining in the 2ME2 (150 mg/kg) treated tumors. Insets: higher magnification.

We next examined the effects of 2ME2 on endothelial cell tubulin *in vivo* (Fig. 230b). Tumor sections from untreated or 2ME2 treated animals were double-labeled with antibodies against α-tubulin (red staining) and CD31 (green staining). Careful examination of the integrity of MTs in CD31 positive endothelial cells revealed MT-disruption in the treated animals compared to the undisturbed MT network in control animals (Fig. 30b, insets).

Together, our *in vivo* data show that at concentrations that inhibit tumor growth and tumor angiogenesis, 2ME2 effectively disrupts tumor microtubules, inhibits tumor vascularization, and downregulates HIF-1α.

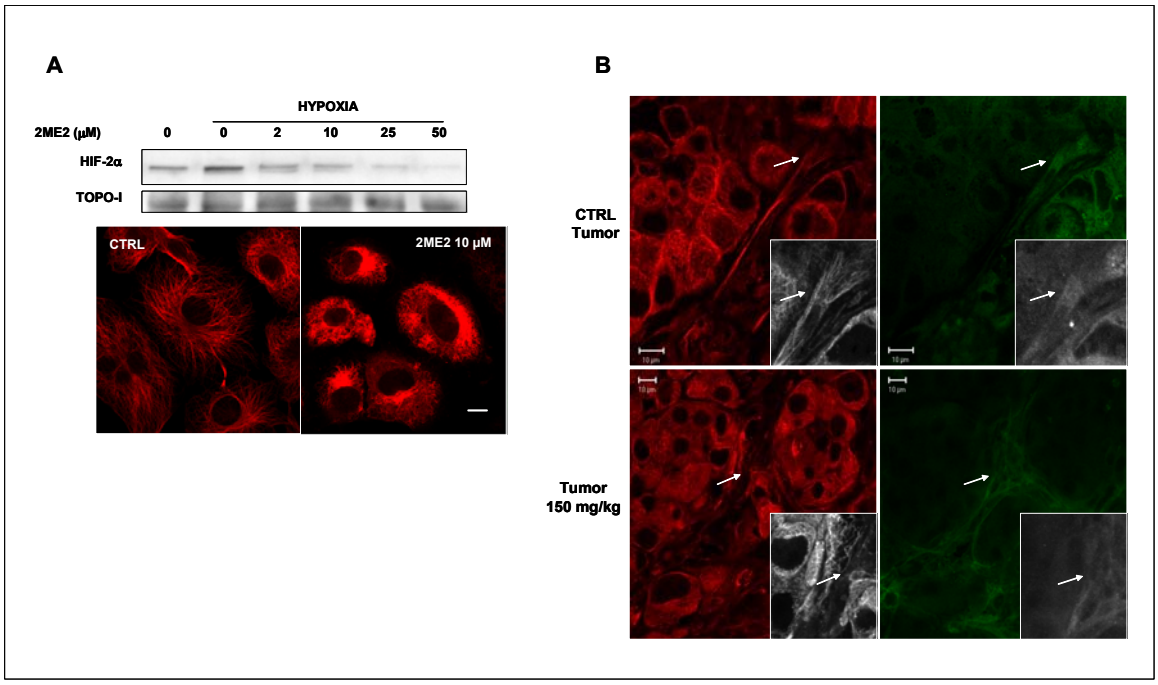

Figure 30. 2ME2 inhibits HIF-2α and depolymerizes microtubules in endothelial cells. A: HUVEC cells were treated with 2ME2, and processed for HIF-2α Western blotting (upper panel) and confocal microscopy for tubulin staining (lower panel). Scale bar, 10 μm**. B:** Double labeling immunofluorescence staining with antibodies against α-tubulin (red) and antCD31 (white) was performed in tumor sections from treated an untreated animals. Arrows depict MTs in endothelial cells. Insets show higher magnification of endothelial cell tubulin. Notice the well organized MT network of endothelial cells in the untreated tumor *versus* the depolymerized MTs observed in endothelial cells in the 2ME2 treated tumors.

DISCUSSION

Angiogenesis is one of the important biological processes required to support tumor growth beyond a certain threshold size. Therefore, the development of angiogenesis inhibitors has recently become an attractive new strategy to combat cancer. In this study, we have identified a novel molecular mechanism by which 2ME2, an antitumor agent and angiogenesis inhibitor currently in Phase I/II trials, exerts its activity. Our results show that 2ME2 depolymerizes MTs, downregulates HIF-1α protein levels and HIF transcriptional activity in an oxygen- and proteasome-independent manner (Figs. 1 and 3). Most importantly, we demonstrate that at concentrations that inhibit tumor growth and vascularization *in vivo*, 2ME2 effectively depolymerizes tumor MTs.

In vitro, 2ME2 has been shown to compete with colchicine for tubulin binding and to disrupt interphase MTs leading to mitotic arrest and cell death in cultured cancer cells [166, 186, 187]. In addition, when we treated human endothelial cells (HUVEC) with 2ME2 we observed a dose dependent MT-depolymerization at concentrations similar to those used in tumor cells (Fig. 5e). The antiangiogenic properties of this compound, however, had not been correlated previously with its effects on MTs. Other MT-targeting compounds have also been shown to possess varying degrees of antiangiogenic activity, including the colchicine-site agents combretastatins, [188-190] and ZD6126 [191] and the taxane-site agents, such as Taxol, [164, 192] docetaxel [193] and IDN 5390 [194]. The above studies led to the hypothesis that the antivascular effects of MT-targeting agents derive from their ability to selectively inhibit the growth of endothelial cells in tumor vessels, producing vascular shutdown and massive tumor necrosis. Our data show that 2ME2 affects *in vivo* tubulin in both the tumor and endothelial cell compartments (Fig. 5f), which suggests that 2ME2 may interfere with the cross-talk between cancer and endothelial cells further contributing to the antitumor and anti-angiogenic activity of 2ME2.

Decreased VEGF protein levels after 2ME2 treatment have been reported previously, [195, 196] however, the molecular mechanism responsible for this decrease had not been identified. Our data show that 2ME2 interferes with the downstream activation of HIF-1 target genes in response to hypoxia, only one of which is VEGF (Fig. 2). Thus, our current hypothesis is that the antitumor/antiangiogenic activity of 2ME2 likely results from both the inhibition of the normal function of tumor MTs and the inhibition of the HIF-transcriptome. This hypothesis is supported by data in the literature showing that inhibition of VEGF *in vivo*, by the recombinant humanized antibody directed against VEGF (rhuMAb-VEGF) led to only a 25% inhibition of angiogenesis,

whereas 2ME2 inhibited angiogenesis by 63% [193]. This result is in agreement with our *in vivo* data where a 64% inhibition of angiogenesis was obtained after treatment with 150 mg/kg 2ME2 (Fig. 5), and it further suggests that the 2ME2 antiangiogenic activity might not be solely attributed to inhibition of VEGF. While we have not been able to confirm all of our *in vitro* observations *in vivo*, our data support the hypothesis that 2ME2 affects MTs and its downstream effects on HIF pathway lead to inhibition of tumor vascularization *in vivo*. We believe further studies using human cancer cells lacking HIF-1 and HIF-2 activity are warranted to conclusively elucidate the important steps involved in this process *in vivo*.

In our experiments, we have demonstrated that Taxol and vincristine also inhibited HIF-1α levels and HIF-1 transcriptional activity (Fig.3*b* & *c*). We further showed that this effect is not a consequence of mitotic arrest since monastrol, a non MT-targeting drug that induces mitotic arrest, [183] was not able to downregulate HIF-1 levels (Fig. 3d). We have also demonstrated that the alterations in the MT-cytoskeleton, resulting from the interaction of the MT-targeting drugs with tubulin, is required for the inhibition of HIF (Fig. 4). However, we have not yet determined what the signaling events are that link MT disruption to HIF-1α inhibition. Interestingly, a recent study has shown that VHL is a tubulin associated protein that helps stabilize interphase microtubules potentially identifying a new role for pVHL function in VHL disease [129]. However, how the pVHL stabilizing effects on MTs may be linked to the VHL-HIF functional regulation is currently unclear [197]. Future studies are warranted to increase our understanding of the molecular mechanisms that regulate these pathways.

Taken together, our results show that disruption of interphase MTs results in repression of HIF-1α, likely at the level of translation, which in turn leads to inhibition of HIF-1 transcriptional activity, including downregulation of VEGF expression. We have further determined that inhibition of HIF-1α by 2ME2 or other MT-targeting compounds occurs downstream of drug-tubulin interaction. This finding provides mechanistic insight into the anti-angiogenic mechanism of action reported for several MT-targeting compounds and supports the hypothesis that tubulin-targeting drugs inhibit both tumor cell growth and tumor vascularization following disruption of the MT-cytoskeleton. The further characterization of the molecular signals linking the disruption of the MT-cytoskeleton with the downregulation of HIF-mediated angiogenesis, are likely to identify novel targets for the development of new anticancer therapies.

2ME2 is currently in Phase I/II clinical trials in breast, metastatic breast and prostate cancer. The preliminary results from these trials show promising responses without any serious drug-related adverse effects even when 2ME2 is administered at doses of 1,000-1,200 mg/day [198]. Herein, we show that 2ME2 is a lead compound that has a dual effect on MTs, a validated anticancer drug target, and HIF, which we believe it is an important survival factor in cancer.

CONCLUSIONS

In this work we sought to understand the molecular details underlying the antitumor and antiangiogenic properties of 2ME2. Our objectives were to characterize the molecular mechanisms by which 2ME2 inhibits HIF-1 and angiogenesis, and to analyze whether there was a cause-and-effect relationship between 2ME2's antiangiogenic and anti-tubulin properties. The major conclusions of this work are:

1. Mechanistically 2ME2 downregulates the hypoxia-inducible factor-1 (HIF) at the post-transcriptional level, and inhibits HIF-1-induced transcriptional activation of VEGF expression.
2. 2ME2 does not induce proteasomal degradation of HIF-1 nor does it reduce HIF-1 mRNA levels, but rather inhibits the *de novo* HIF-1 protein synthesis.
3. Inhibition of HIF-1 occurs downstream of the 2ME2/tubulin interaction, as disruption of interphase microtubules is required for HIF-α downregulation.
4. At concentrations that have antiproliferative activity *in vitro*, 2ME2 blocks HIF-1α nuclear accumulation and HIF-1 activity by an oxygen- and proteasome-independent pathway.
5. Our findings demonstrate for the first time that 2ME2 destabilizes microtubules at doses that are efficacious *in vivo*.
6. The effects of 2ME2 on microtubules are not unique but rather shared with other microtubule-targeting drugs, such as Taxol and Vincristine. Thus, this mechanism may explain the antiangiogenic activities
7. Our work establishes 2ME2 as a new small molecule inhibitor of HIF-1, and provides a mechanistic link between the disruption of the microtubule-cytoskeleton and inhibition of angiogenesis.

MATERIALS AND METHODS

Chemicals and antibodies. 2ME2 was purchased from Tetrionics (Madison, WI) and 0.1mM stock solutions were made in DMSO and stored in aliquots at –80^{o}C. The compound was diluted in incubation media immediately prior to each experiment. Thawed stock solutions were used once and discarded. Vincristine was from Eli-Lilly (Indianapolis, Indiana), Paclitaxel and Cyclophosphamide were from Sigma (St Louis, Missouri). MG-132 (Z-Leu--Leu--Leu-aldehyde) was purchased from Alexis Biochemicals (San Diego, California). Monastrol was from AG Scientific, Inc (San Diego, California) The following primary antibodies were used: rat anti α-tubulin (Chemicon International, Temecula, California), mouse anti HIF-1α (BD Biosciences, San Diego, California), rat anti-CD31 (PharMingen, San Diego, California), polyclonal antibody against human HIF-2α and monoclonal HIF-1β (Novus Biologicals, Littleton, Colorado), human actin antibody was from Santa Cruz Biotechnology, Inc. (Santa Cruz, California), polyclonal human antibody to human topoisomerase I (TOPO-I) (TopoGEN, Columbus, Ohio). Rabbit polyclonal antibodies to c-Jun, c-Fos, NF-κB p50, and NF-κB p65 were from Geneka Biotechnology, Inc (Montréal, Québec, Canada). Rabbit polyclonal antibody to c-myc was from Sigma (St Louis, Missouri). Secondary antibodies were horseradish peroxidase-conjugated (Amersham Pharmacia Biotech, Piscataway, New Jersey), Alexa Fluor 488 goat anti-mouse (Molecular Probes, Eugene, Oregon), Alexa Fluor 568 goat anti rat (Molecular Probes, Eugene, Oregon), AlexaFluor 568 goat anti-rabbit (Molecular Probes, Eugene, Oregon), Rhodamine Red-X mouse anti-rat (Jackson ImmunoResearch, West Grove, Baltimore).

Cell lines. Human breast cancer MDA-MB-231 cells were maintained in DMEM and human prostate cancer PC-3 cells, 1A9 human ovarian carcinoma cells and its paclitaxel-resistant subline 1A9/PTX10 were cultured in RPMI 1640; Human Umbilical Vein Endothelial Cells (HUVEC) were cultured in M199 media. All media were supplemented with 10% FBS and antibiotics. Cells were cultured at 37ºC in a humidified atmosphere and 5% CO_2 in air. For hypoxic exposure, cells were placed in a sealed modular incubator chamber (Billups-Rothenberg, Del Mar, California) flushed with 1% O_2, 5% CO_2 and 94% N_2.

Drug treatments / 2ME2 Treatment of Cells. Cells were seeded in culture dishes and grown until 70% confluence. The medium was then replaced with a new medium containing either vehicle (0.1% DMSO) or 2ME2 at the concentrations indicated in the figures for overnight at

37ºC. The following day, cells were exposed to hypoxia or left under normoxia for 6 hours. The cells were then washed twice with ice-cold PBS, harvested and nuclear extract (NE) was prepared as described [199] or alternately a whole cell extract (WCE) was prepared by lysing the cells with 100mM potassium phosphate (pH 7.8) and 0.2% Triton X-100 supplemented with protease and phosphatase inhibitors.

Western blotting. Proteins (50-70μg/lane) from whole cell extracts (WCEs) or nuclear extracts (NE) were resolved by 7.5% SDS-PAGE, electrotransferred to nitrocellulose membrane and incubated with the indicated primary antibodies, followed by horseradish peroxidase-conjugated secondary antiserum. Immunoreactivity was visualized by enhanced chemiluminescence reagent (Amersham Biosciences, Piscataway, New Jersey). For sequential blotting with additional antibodies the membranes were stripped using a restore Western blot stripping buffer (Pierce, Rockford, IL) and re-probed with the indicated antibodies.

ELISA for VEGF. VEGF concentration in media from treated cells was determined using ELISA kit for VEGF protein (R & D Systems, Inc., Minneapolis, MN) according to the manufacturers' instructions. The results were expressed as concentration of VEGF (pg/ml) per the total protein amount from each well.

HRE-luciferase reporter assay. PC3 cells growing in 6-well plates in triplicate were transiently transfected with 1μg/well of the HRE-reporter vector pBI-GL V6L (containing 6 tandem copies of the hypoxia response element of the VEGF gene) [179, 180] using GenePorter transfection reagent (Gene Therapy Sys, Inc., San Diego, CA). After 5 hours of transfection media was supplemented with 10% FBS, and cells were allowed to recover overnight. The cells were then washed twice with PBS and replenished with complete medium containing 10% FBS or 100μM 2ME2 and incubated either under normoxia or hypoxia for 16 hours. Luciferase reporter activity was measured with a commercial kit TROPIX (Bedford, MA) using a BMG Labtechnologies LUMIstar Galaxy Luminometer and following manufacture's instructions. Arbitrary luciferase activity units were normalized to the amount of protein in each assay point. Protein concentration was measured using a BCA protein assay kit (Pierce, Rockford, IL).

Electrophoretic Mobility Shift Assay. EMSA was performed by incubating 5 μg of nuclear extract and oligonucleotide probe W18 in 20 μl of binding buffer as previously described [27]. For supershift analysis, 1 μg of HIF-1α or HIF-2α antibody (Santa Cruz Biotechnology, Inc. Santa Cruz, California) was added to the reaction mixture and incubated for 20 min at 4ºC. For competition experiments, a 100-fold excess of unlabeled annealed oligonucleotide was added to the reaction mixture with the labeled probe.

Isolation and Analysis of RNA. Total RNA was isolated using TRIzol Reagent (Life Technologies, Inc) and Northen Blotting was performed with probes specific for human HIF-1α, VEGF 165, endothelin 1 (ET-1), Glut-1 glucose transporter and β-actin (Ambion, Inc., Austin, Texas) as described. [27]

HIF-1α Protein Translation Assay. PC-3 cells were plated into 6-well plates and grown to 70% confluence. Cells were pretreated overnight with 25μM 2ME2 or DMSO (0.025% vol/vol). Then medium was changed to methionine- and cysteine-free as well as serum-free RPMI 1640 medium for 2 hours. After 2 hours, cells were labeled by incubation with methionine- and cysteine-free medium containing ^{35}S-methionine (ICN Biomedicals, Inc., California) at a final concentration of 100μCi/well at 37ºC for the indicated time in the figure. Subsequently, the cells were washed twice with ice-cold PBS, lysed and subjected for immunoprecipitation using anti-HIF-1α antibody and protein G-agarose beads (Pierce, IL) as previously described. [180]

Pulse Chase Assay. PC-3 cells grown in 6-well plates were labeled with ^{35}S-methionine as described above. The radioactive medium was then removed and cells were re-cultured in complete medium with 0.1%DMSO or 100μM 2ME2 for various times. Subsequently, the cells were washed twice with ice-cold PBS, lysed and subjected for immunoprecipitation using anti-HIF-1α antibody as previously described [180].

Ubiquitination Assay. A plasmid was constructed containing p3xFLAG-myc-CMV-25 (Sigma) with a coding sequence HIF-1α cDNA inserted into the HindIII/NotI site. Cells were transiently transfected with the plasmid for 24 h and then treated with vehicle or 50□M 2ME2. The cells were collected and lysed in 50 mM Tris HCl, pH 7.4, 150 mM NaCl, 1mM EDTA, 1% Triton X-

100. Immunoprecipitation was performed with anti-FLAG M2 affinity gels (Sigma). The samples were boiled in SDS sample buffer, and analyzed by SDS-PAGE and immunoblotted with and rabbit polyclonal ubiquitin antibody (Santa Cruz).

Tumor Models and Immunohistochemistry. Female 8-10 week-old BALB/c nu/nu mice (Jackson Laboratories, Bar Harbor, ME) were injected in the mammary fat pad with $2x10^6$ MDA-MB-231 cells. Daily orally administration of 2ME2 was initiated when the tumors became palpable (4-5 mm diameter) on day 20 after implantation. A suspension of 2ME2 was prepared by homogenization in an aqueous solution of 0.5% methylcellulose (Sigma, St Louis, Missouri) using a Kinematica polytron (Brinkmann, Westbury, New York). At the end of the dosing regimen on day 53 (treatment duration was 33 days) animals were sacrifised and tumor volumes were calculated as $width^2$ x length x 0.52. Upon termination of the dosing regimen, animals were euthanized with 20 mg/100 g BW of phenobarbital (Sigma, St Louis, Missouri) and tumors were excised as quickly as possible and cut into 1 mm^2 pieces. One piece of tumor was dounced and placed into 200 µl of microtubule-stabilizing buffer and processed for the tubulin polymerization assay (for details see below). The rest of tumor pieces were fixed with 3.7% formaldehyde, 0.05% glutaraldehyde and 0.5 % Triton X-100 in PHEMO buffer for 30 min at room temperature. Then they were transferred into 4% formaldehyde in 0.1 M sodium cacodylate buffer (Sigma, St Louis, Missouri) pH 7.3 for an additional 4 hr. Tumor pieces were stored at 4^oC in the same buffer until they were immunostained for α-tubulin as described above, and CD-31.

Immunohistochemical Determination of CD 31/PECAM-1

For immunohistochemistry, tumors were fixed in 10% buffered formalin (Sigma). Paraffin embedded tissue was sectioned at 5µm and mounted on Superfrost slides (Fisher Scientific, Co., Houston TX). Sections were deparaffinized in xylene, subsequently immersed in graded alcohol (100%, 95% ethanol) rehydrated in ddH_2O and Tris buffer. Sections were then treated with Protinase K (Roche Indianapolis, IN), washed in Tris-buffer, blocked for endogenous peroxidase activity by use of 3% hydrogen peroxide in methanol for 20 minutes. After blocking sections with TNB block for 45 minutes (NEN Life Science Products, Inc. Boston MA) sections were incubated with primary antibody at 4°C overnight (CD 31 at 1:250 dilution) rat anti-mouse

antibody (PharMingen, San Diego, CA). Slides were then washed TNT wash buffer (NEN), incubated with species-specific biotinylated secondary antibody for 30 minutes (1:200 dilution, Vector Laboratories, Burlingame, CA). After secondary incubation slides were washed in TNT buffer, sections were amplified with tyramide-horderdase peroxidase (NEN) and visualized by incubating the slides with 3, 3'-diaminobenzidine (Vector). The slides were counterstained with Gills Hemotoxylin III (Sigma, St. Louis, MO), rinsed and immersed briefly in 1% ammonia solution for nuclei binding. Finally, slides were hydrated and mounted with cytoseal (VWR International, West Chester, PA) and covered with Fisherfinest glass cover slips (Fisher). For negative controls the exact procedure was done with either the omission of the primary antibody or the secondary.

Quantification of MVD.

For quantification of CD31, tumor sections that stained positive for CD31 vessels were used in the analysis. Microvasular density (MVD) was measured by using Bioquant Image Analysis System (PAI, Frederick MA). To quantify the vessels, 10 areas at 168 μm^2 per field at x 200 were captured for each tumor using Olympus BX 40 microscope.

Immunofluorescence and Confocal Microscopy.

A. Cell Lines. Exponentially growing cells were plated on 12-mm glass coverslips (Fisher Scientific, Pittsburgh, Pennsylvania) into 24-well plates and cells were allowed to attach overnight. The following day, cells were treated with the indicated drugs for 16 h and subjected to hypoxia for an additional 6 hours. Cells were fixed with PHEMO buffer (PIPES 0.068M, HEPES 0.025 M, EGTA 0.015 M, MgCl2 0.003 M, 10% DMSO, pH, 6.8) containing 3.7 % formaldehyde, 0.05% glutaraldehyde, 0.5 % Triton X-100, for 10min at room temperature. Coverslips were blocked in 10% goat serum in PBS for 10min and processed for double-labeling immunofluorescence with rat anti-α-tubulin, mouse anti HIF-1α and mouse anti HIF-1β antibodies. The secondary antibodies were Alexa Fluor 488 goat anti-mouse antibody and Alexa Fluor 568 goat anti-rat antibody antibodies. Coverslips were then mounted onto glass slides and examined with a LSM510 META Zeiss axioplasm laser scanning confocal microscope.

B. Tumor sections**.** Animals were treated as described above. For tubulin immunofluorescence followed by LSCM, $1mm^2$ pieces of tumor from each animal were fixed in PHEMO buffer

containing 3.7 % formaldehyde, 0.05% glutaraldehyde, 0.5 % Triton X-100, for 1-2 h at room temperature. Following fixation tumor pieces were stored in 4% paraformaldehyde in 0.1. % sodium cacodylate at 4^0C for up to a month before further processing. Fixed tumor sections were embedded in low-melting agarose (Sigma, St Louis, Missouri) and 50 μm sections were obtained by vibratome sectioning at low speed (Vibratome Series 1000 Sectioning System) as previously described. [200] Sections were then processed for α-tubulin immunofluorescence staining and laser scanning confocal microscopy as described above.

Tubulin Polymerization Assay. The percent of polymerized tubulin from the tumors of the treated animals was by douncing a piece tumor for each animal placing assessed as previously described [185] with some modifications. A piece of tumor from each animal was chopped and placed placed into 200 μl of MT-stabilizing buffer (0.1M PIPES, 1mM EGTA, 1mM $MgSO_4$, 30% glycerol and 5% DMSO, pH 6.9) supplemented with protease inhibitors cocktail. The tissue was then placed immediately at 37^oC for 5 min to allow tubulin polymerization to occur, and centrifugated at room temperature at 20,000 x g for 10 min. Equal amounts of the supernatant and the pellet fraction were resolved were analyzed by SDS-PAGE and immunoblotted with an antibody against α-tubulin.

Data Analysis. Experiments presented in the figures are representative of 3 or more different repetitions. Quantification of band densities was performed using the public domain NIH Image (version 1.61). Statistical analysis was performed using a one-way ANOVA test ($P < 0.05$ was considered statistically significant).

REFERENCES

1. Pribluda, V.S., Gubish, E.R., Jr., Lavallee, T.M., Treston, A., Swartz, G.M., and Green, S.J. (2000). 2-Methoxyestradiol: an endogenous antiangiogenic and antiproliferative drug candidate. Cancer Metastasis Rev *19*, 173-179.
2. Tozer, G.M., Kanthou, C., Parkins, C.S., and Hill, S.A. (2002). The biology of the combretastatins as tumour vascular targeting agents. Int J Exp Pathol *83*, 21-38.
3. Folkman, J. (2001). Angiogenesis-dependent diseases. Semin Oncol *28*, 536-542.
4. Goldman, E. (1907). The growth of malignant disease in man and the lower animals with special reference to the vascular system. Lancet *2*, 1236-1240.
5. Folkman, J. (1971). Tumor angiogenesis: therapeutic implications. N Engl J Med *285*, 1182-1186.
6. Heissig, B., Hattori, K., Friedrich, M., Rafii, S., and Werb, Z. (2003). Angiogenesis: vascular remodeling of the extracellular matrix involves metalloproteinases. Curr Opin Hematol *10*, 136-141.
7. Visse, R., and Nagase, H. (2003). Matrix metalloproteinases and tissue inhibitors of metalloproteinases: structure, function, and biochemistry. Circ Res *92*, 827-839.
8. Carmeliet, P., Ferreira, V., Breier, G., Pollefeyt, S., Kieckens, L., Gertsenstein, M., Fahrig, M., Vandenhoeck, A., Harpal, K., Eberhardt, C., Declercq, C., Pawling, J., Moons, L., Collen, D., Risau, W., and Nagy, A. (1996). Abnormal blood vessel development and lethality in embryos lacking a single VEGF allele. Nature *380*, 435-439.
9. Ferrara, N., Carver-Moore, K., Chen, H., Dowd, M., Lu, L., O'Shea, K.S., Powell-Braxton, L., Hillan, K.J., and Moore, M.W. (1996). Heterozygous embryonic lethality induced by targeted inactivation of the VEGF gene. Nature *380*, 439-442.
10. Tischer, E., Mitchell, R., Hartman, T., Silva, M., Gospodarowicz, D., Fiddes, J.C., and Abraham, J.A. (1991). The human gene for vascular endothelial growth factor. Multiple protein forms are encoded through alternative exon splicing. J Biol Chem *266*, 11947-11954.
11. Soker, S., Takashima, S., Miao, H.Q., Neufeld, G., and Klagsbrun, M. (1998). Neuropilin-1 is expressed by endothelial and tumor cells as an isoform-specific receptor for vascular endothelial growth factor. Cell *92*, 735-745.
12. Suri, C., Jones, P.F., Patan, S., Bartunkova, S., Maisonpierre, P.C., Davis, S., Sato, T.N., and Yancopoulos, G.D. (1996). Requisite role of angiopoietin-1, a ligand for the TIE2 receptor, during embryonic angiogenesis. Cell *87*, 1171-1180.
13. Holash, J., Wiegand, S.J., and Yancopoulos, G.D. (1999). New model of tumor angiogenesis: dynamic balance between vessel regression and growth mediated by angiopoietins and VEGF. Oncogene *18*, 5356-5362.
14. Hata, Y., Rook, S.L., and Aiello, L.P. (1999). Basic fibroblast growth factor induces expression of VEGF receptor KDR through a protein kinase C and p44/p42 mitogen-activated protein kinase-dependent pathway. Diabetes *48*, 1145-1155.
15. Bussolino, F., Albini, A., Camussi, G., Presta, M., Viglietto, G., Ziche, M., and Persico, G. (1996). Role of soluble mediators in angiogenesis. Eur J Cancer *32A*, 2401-2412.
16. Bredel, M., Pollack, I.F., Campbell, J.W., and Hamilton, R.L. (1997). Basic fibroblast growth factor expression as a predictor of prognosis in pediatric high-grade gliomas. Clin Cancer Res *3*, 2157-2164.
17. Stupack, D.G., and Cheresh, D.A. (2003). Apoptotic cues from the extracellular matrix: regulators of angiogenesis. Oncogene *22*, 9022-9029.

18. Chan, B.M., Matsuura, N., Takada, Y., Zetter, B.R., and Hemler, M.E. (1991). In vitro and in vivo consequences of VLA-2 expression on rhabdomyosarcoma cells. Science *251*, 1600-1602.
19. Bohm, M., Totzeck, B., Birchmeier, W., and Wieland, I. (1994). Differences of E-cadherin expression levels and patterns in primary and metastatic human lung cancer. Clin Exp Metastasis *12*, 55-62.
20. Liekens, S., De Clercq, E., and Neyts, J. (2001). Angiogenesis: regulators and clinical applications. Biochem Pharmacol *61*, 253-270.
21. Stromblad, S., Becker, J.C., Yebra, M., Brooks, P.C., and Cheresh, D.A. (1996). Suppression of p53 activity and p21WAF1/CIP1 expression by vascular cell integrin alphaVbeta3 during angiogenesis. J Clin Invest *98*, 426-433.
22. Gray, L.H., Conger, A.D., Ebert, M., Hornsey, S., and Scott, O.C. (1953). The concentration of oxygen dissolved in tissues at the time of irradiation as a factor in radiotherapy. Br J Radiol *26*, 638-648.
23. Vaupel, P. (1993). Oxygenation of solid tumors. In Drug Resistance in Oncology, B.A. Teicher, ed. (New York: Marcel Dekker), pp. 53-85.
24. Warburg, O. (1956). [Origin of cancer cells]. Oncologia *9*, 75-83.
25. Brown, J.M., and Wilson, W.R. (2004). Exploiting tumour hypoxia in cancer treatment. Nat Rev Cancer *4*, 437-447.
26. Comerford, K.M., Wallace, T.J., Karhausen, J., Louis, N.A., Montalto, M.C., and Colgan, S.P. (2002). Hypoxia-inducible factor-1-dependent regulation of the multidrug resistance (MDR1) gene. Cancer Res *62*, 3387-3394.
27. Wang, G.L., Jiang, B.H., Rue, E.A., and Semenza, G.L. (1995). Hypoxia-inducible factor 1 is a basic-helix-loop-helix-PAS heterodimer regulated by cellular O2 tension. Proc Natl Acad Sci U S A *92*, 5510-5514.
28. Tian, H., McKnight, S.L., and Russell, D.W. (1997). Endothelial PAS domain protein 1 (EPAS1), a transcription factor selectively expressed in endothelial cells. Genes Dev *11*, 72-82.
29. Ema, M., Taya, S., Yokotani, N., Sogawa, K., Matsuda, Y., and Fujii-Kuriyama, Y. (1997). A novel bHLH-PAS factor with close sequence similarity to hypoxia-inducible factor 1alpha regulates the VEGF expression and is potentially involved in lung and vascular development. Proc Natl Acad Sci U S A *94*, 4273-4278.
30. Flamme, I., Frohlich, T., von Reutern, M., Kappel, A., Damert, A., and Risau, W. (1997). HRF, a putative basic helix-loop-helix-PAS-domain transcription factor is closely related to hypoxia-inducible factor-1 alpha and developmentally expressed in blood vessels. Mech Dev *63*, 51-60.
31. Hogenesch, J.B., Chan, W.K., Jackiw, V.H., Brown, R.C., Gu, Y.Z., Pray-Grant, M., Perdew, G.H., and Bradfield, C.A. (1997). Characterization of a subset of the basic-helix-loop-helix-PAS superfamily that interacts with components of the dioxin signaling pathway. J Biol Chem *272*, 8581-8593.
32. Gu, Y.Z., Moran, S.M., Hogenesch, J.B., Wartman, L., and Bradfield, C.A. (1998). Molecular characterization and chromosomal localization of a third alpha-class hypoxia inducible factor subunit, HIF3alpha. Gene Expr *7*, 205-213.
33. Hara, S., Hamada, J., Kobayashi, C., Kondo, Y., and Imura, N. (2001). Expression and characterization of hypoxia-inducible factor (HIF)-3alpha in human kidney: suppression

of HIF-mediated gene expression by HIF-3alpha. Biochem Biophys Res Commun *287*, 808-813.

34. Makino, Y., Cao, R., Svensson, K., Bertilsson, G., Asman, M., Tanaka, H., Cao, Y., Berkenstam, A., and Poellinger, L. (2001). Inhibitory PAS domain protein is a negative regulator of hypoxia-inducible gene expression. Nature *414*, 550-554.
35. Jain, S., Maltepe, E., Lu, M.M., Simon, C., and Bradfield, C.A. (1998). Expression of ARNT, ARNT2, HIF1 alpha, HIF2 alpha and Ah receptor mRNAs in the developing mouse. Mech Dev *73*, 117-123.
36. Wiener, C.M., Booth, G., and Semenza, G.L. (1996). In vivo expression of mRNAs encoding hypoxia-inducible factor 1. Biochem Biophys Res Commun *225*, 485-488.
37. Peng, J., Zhang, L., Drysdale, L., and Fong, G.H. (2000). The transcription factor EPAS-1/hypoxia-inducible factor 2alpha plays an important role in vascular remodeling. Proc Natl Acad Sci U S A *97*, 8386-8391.
38. Tian, H., Hammer, R.E., Matsumoto, A.M., Russell, D.W., and McKnight, S.L. (1998). The hypoxia-responsive transcription factor EPAS1 is essential for catecholamine homeostasis and protection against heart failure during embryonic development. Genes Dev *12*, 3320-3324.
39. Iyer, N.V., Kotch, L.E., Agani, F., Leung, S.W., Laughner, E., Wenger, R.H., Gassmann, M., Gearhart, J.D., Lawler, A.M., Yu, A.Y., and Semenza, G.L. (1998). Cellular and developmental control of O2 homeostasis by hypoxia- inducible factor 1 alpha. Genes Dev *12*, 149-162.
40. Ryan, H.E., Lo, J., and Johnson, R.S. (1998). HIF-1 alpha is required for solid tumor formation and embryonic vascularization. Embo J *17*, 3005-3015.
41. Jaakkola, P., Mole, D.R., Tian, Y.M., Wilson, M.I., Gielbert, J., Gaskell, S.J., Kriegsheim, A., Hebestreit, H.F., Mukherji, M., Schofield, C.J., Maxwell, P.H., Pugh, C.W., and Ratcliffe, P.J. (2001). Targeting of HIF-alpha to the von Hippel-Lindau ubiquitylation complex by O2-regulated prolyl hydroxylation. Science *292*, 468-472.
42. Ivan, M., Kondo, K., Yang, H., Kim, W., Valiando, J., Ohh, M., Salic, A., Asara, J.M., Lane, W.S., and Kaelin, W.G., Jr. (2001). HIFalpha targeted for VHL-mediated destruction by proline hydroxylation: implications for O2 sensing. Science *292*, 464-468.
43. Masson, N., Willam, C., Maxwell, P.H., Pugh, C.W., and Ratcliffe, P.J. (2001). Independent function of two destruction domains in hypoxia-inducible factor-alpha chains activated by prolyl hydroxylation. Embo J *20*, 5197-5206.
44. Epstein, A.C., Gleadle, J.M., McNeill, L.A., Hewitson, K.S., O'Rourke, J., Mole, D.R., Mukherji, M., Metzen, E., Wilson, M.I., Dhanda, A., Tian, Y.M., Masson, N., Hamilton, D.L., Jaakkola, P., Barstead, R., Hodgkin, J., Maxwell, P.H., Pugh, C.W., Schofield, C.J., and Ratcliffe, P.J. (2001). C. elegans EGL-9 and mammalian homologs define a family of dioxygenases that regulate HIF by prolyl hydroxylation. Cell *107*, 43-54.
45. Bruick, R.K., and McKnight, S.L. (2001). A conserved family of prolyl-4-hydroxylases that modify HIF. Science *294*, 1337-1340.
46. Jeong, J.W., Bae, M.K., Ahn, M.Y., Kim, S.H., Sohn, T.K., Bae, M.H., Yoo, M.A., Song, E.J., Lee, K.J., and Kim, K.W. (2002). Regulation and destabilization of HIF-1alpha by ARD1-mediated acetylation. Cell *111*, 709-720.
47. Lando, D., Peet, D.J., Gorman, J.J., Whelan, D.A., Whitelaw, M.L., and Bruick, R.K. (2002). FIH-1 is an asparaginyl hydroxylase enzyme that regulates the transcriptional activity of hypoxia-inducible factor. Genes Dev *16*, 1466-1471.

48. Cress, W.D., and Seto, E. (2000). Histone deacetylases, transcriptional control, and cancer. J Cell Physiol *184*, 1-16.
49. Semenza, G.L. (2003). Targeting HIF-1 for cancer therapy. Nat Rev Cancer *3*, 721-732.
50. Harris, A.L. (2002). Hypoxia--a key regulatory factor in tumour growth. Nat Rev Cancer *2*, 38-47.
51. Semenza, G. (2002). Signal transduction to hypoxia-inducible factor 1. Biochem Pharmacol *64*, 993-998.
52. Richard, D.E., Berra, E., Gothie, E., Roux, D., and Pouyssegur, J. (1999). p42/p44 mitogen-activated protein kinases phosphorylate hypoxia-inducible factor 1alpha (HIF-1alpha) and enhance the transcriptional activity of HIF-1. J Biol Chem *274*, 32631-32637.
53. Sodhi, A., Montaner, S., Patel, V., Zohar, M., Bais, C., Mesri, E.A., and Gutkind, J.S. (2000). The Kaposi's sarcoma-associated herpes virus G protein-coupled receptor up-regulates vascular endothelial growth factor expression and secretion through mitogen-activated protein kinase and p38 pathways acting on hypoxia-inducible factor 1alpha. Cancer Res *60*, 4873-4880.
54. Park, J.H., Kim, T.Y., Jong, H.S., Chun, Y.S., Park, J.W., Lee, C.T., Jung, H.C., Kim, N.K., and Bang, Y.J. (2003). Gastric epithelial reactive oxygen species prevent normoxic degradation of hypoxia-inducible factor-1alpha in gastric cancer cells. Clin Cancer Res *9*, 433-440.
55. Brune, B., and Zhou, J. (2003). The role of nitric oxide (NO) in stability regulation of hypoxia inducible factor-1alpha (HIF-1alpha). Curr Med Chem *10*, 845-855.
56. Chandel, N.S., McClintock, D.S., Feliciano, C.E., Wood, T.M., Melendez, J.A., Rodriguez, A.M., and Schumacker, P.T. (2000). Reactive oxygen species generated at mitochondrial complex III stabilize hypoxia-inducible factor-1alpha during hypoxia: a mechanism of O2 sensing. J Biol Chem *275*, 25130-25138.
57. Zhong, H., De Marzo, A.M., Laughner, E., Lim, M., Hilton, D.A., Zagzag, D., Buechler, P., Isaacs, W.B., Semenza, G.L., and Simons, J.W. (1999). Overexpression of hypoxia-inducible factor 1alpha in common human cancers and their metastases. Cancer Res *59*, 5830-5835.
58. Talks, K.L., Turley, H., Gatter, K.C., Maxwell, P.H., Pugh, C.W., Ratcliffe, P.J., and Harris, A.L. (2000). The expression and distribution of the hypoxia-inducible factors HIF-1alpha and HIF-2alpha in normal human tissues, cancers, and tumor-associated macrophages. Am J Pathol *157*, 411-421.
59. Birner, P., Gatterbauer, B., Oberhuber, G., Schindl, M., Rossler, K., Prodinger, A., Budka, H., and Hainfellner, J.A. (2001). Expression of hypoxia-inducible factor-1 alpha in oligodendrogliomas: its impact on prognosis and on neoangiogenesis. Cancer *92*, 165-171.
60. Bos, R., Zhong, H., Hanrahan, C.F., Mommers, E.C., Semenza, G.L., Pinedo, H.M., Abeloff, M.D., Simons, J.W., van Diest, P.J., and van der Wall, E. (2001). Levels of hypoxia-inducible factor-1 alpha during breast carcinogenesis. J Natl Cancer Inst *93*, 309-314.
61. Bos, R., van der Groep, P., Greijer, A.E., Shvarts, A., Meijer, S., Pinedo, H.M., Semenza, G.L., van Diest, P.J., and van der Wall, E. (2003). Levels of hypoxia-inducible factor-1alpha independently predict prognosis in patients with lymph node negative breast carcinoma. Cancer *97*, 1573-1581.

62. Schindl, M., Schoppmann, S.F., Samonigg, H., Hausmaninger, H., Kwasny, W., Gnant, M., Jakesz, R., Kubista, E., Birner, P., and Oberhuber, G. (2002). Overexpression of hypoxia-inducible factor 1alpha is associated with an unfavorable prognosis in lymph node-positive breast cancer. Clin Cancer Res *8*, 1831-1837.
63. Sivridis, E., Giatromanolaki, A., Gatter, K.C., Harris, A.L., and Koukourakis, M.I. (2002). Association of hypoxia-inducible factors 1alpha and 2alpha with activated angiogenic pathways and prognosis in patients with endometrial carcinoma. Cancer *95*, 1055-1063.
64. Aebersold, D.M., Burri, P., Beer, K.T., Laissue, J., Djonov, V., Greiner, R.H., and Semenza, G.L. (2001). Expression of hypoxia-inducible factor-1alpha: a novel predictive and prognostic parameter in the radiotherapy of oropharyngeal cancer. Cancer Res *61*, 2911-2916.
65. Koukourakis, M.I., Giatromanolaki, A., Skarlatos, J., Corti, L., Blandamura, S., Piazza, M., Gatter, K.C., and Harris, A.L. (2001). Hypoxia inducible factor (HIF-1a and HIF-2a) expression in early esophageal cancer and response to photodynamic therapy and radiotherapy. Cancer Res *61*, 1830-1832.
66. Kurokawa, T., Miyamoto, M., Kato, K., Cho, Y., Kawarada, Y., Hida, Y., Shinohara, T., Itoh, T., Okushiba, S., Kondo, S., and Katoh, H. (2003). Overexpression of hypoxia-inducible-factor 1alpha(HIF-1alpha) in oesophageal squamous cell carcinoma correlates with lymph node metastasis and pathologic stage. Br J Cancer *89*, 1042-1047.
67. Hui, E.P., Chan, A.T., Pezzella, F., Turley, H., To, K.F., Poon, T.C., Zee, B., Mo, F., Teo, P.M., Huang, D.P., Gatter, K.C., Johnson, P.J., and Harris, A.L. (2002). Coexpression of hypoxia-inducible factors 1alpha and 2alpha, carbonic anhydrase IX, and vascular endothelial growth factor in nasopharyngeal carcinoma and relationship to survival. Clin Cancer Res *8*, 2595-2604.
68. Kuwai, T., Kitadai, Y., Tanaka, S., Onogawa, S., Matsutani, N., Kaio, E., Ito, M., and Chayama, K. (2003). Expression of hypoxia-inducible factor-1alpha is associated with tumor vascularization in human colorectal carcinoma. Int J Cancer *105*, 176-181.
69. Birner, P., Schindl, M., Obermair, A., Breitenecker, G., and Oberhuber, G. (2001). Expression of hypoxia-inducible factor 1alpha in epithelial ovarian tumors: its impact on prognosis and on response to chemotherapy. Clin Cancer Res *7*, 1661-1668.
70. Beasley, N.J., Leek, R., Alam, M., Turley, H., Cox, G.J., Gatter, K., Millard, P., Fuggle, S., and Harris, A.L. (2002). Hypoxia-inducible factors HIF-1alpha and HIF-2alpha in head and neck cancer: relationship to tumor biology and treatment outcome in surgically resected patients. Cancer Res *62*, 2493-2497.
71. Koukourakis, M.I., Giatromanolaki, A., Sivridis, E., Simopoulos, C., Turley, H., Talks, K., Gatter, K.C., and Harris, A.L. (2002). Hypoxia-inducible factor (HIF1A and HIF2A), angiogenesis, and chemoradiotherapy outcome of squamous cell head-and-neck cancer. Int J Radiat Oncol Biol Phys *53*, 1192-1202.
72. Volm, M., and Koomagi, R. (2000). Hypoxia-inducible factor (HIF-1) and its relationship to apoptosis and proliferation in lung cancer. Anticancer Res *20*, 1527-1533.
73. Giatromanolaki, A., Koukourakis, M.I., Sivridis, E., Turley, H., Talks, K., Pezzella, F., Gatter, K.C., and Harris, A.L. (2001). Relation of hypoxia inducible factor 1 alpha and 2 alpha in operable non-small cell lung cancer to angiogenic/molecular profile of tumours and survival. Br J Cancer *85*, 881-890.

74. Burri, P., Djonov, V., Aebersold, D.M., Lindel, K., Studer, U., Altermatt, H.J., Mazzucchelli, L., Greiner, R.H., and Gruber, G. (2003). Significant correlation of hypoxia-inducible factor-1alpha with treatment outcome in cervical cancer treated with radical radiotherapy. Int J Radiat Oncol Biol Phys *56*, 494-501.
75. Birner, P., Schindl, M., Obermair, A., Plank, C., Breitenecker, G., and Oberhuber, G. (2000). Overexpression of hypoxia-inducible factor 1alpha is a marker for an unfavorable prognosis in early-stage invasive cervical cancer. Cancer Res *60*, 4693-4696.
76. Bachtiary, B., Schindl, M., Potter, R., Dreier, B., Knocke, T.H., Hainfellner, J.A., Horvat, R., and Birner, P. (2003). Overexpression of hypoxia-inducible factor 1alpha indicates diminished response to radiotherapy and unfavorable prognosis in patients receiving radical radiotherapy for cervical cancer. Clin Cancer Res *9*, 2234-2240.
77. Haugland, H.K., Vukovic, V., Pintilie, M., Fyles, A.W., Milosevic, M., Hill, R.P., and Hedley, D.W. (2002). Expression of hypoxia-inducible factor-1alpha in cervical carcinomas: correlation with tumor oxygenation. Int J Radiat Oncol Biol Phys *53*, 854-861.
78. Zundel, W., Schindler, C., Haas-Kogan, D., Koong, A., Kaper, F., Chen, E., Gottschalk, A.R., Ryan, H.E., Johnson, R.S., Jefferson, A.B., Stokoe, D., and Giaccia, A.J. (2000). Loss of PTEN facilitates HIF-1-mediated gene expression. Genes Dev *14*, 391-396.
79. Jiang, B.H., Jiang, G., Zheng, J.Z., Lu, Z., Hunter, T., and Vogt, P.K. (2001). Phosphatidylinositol 3-kinase signaling controls levels of hypoxia-inducible factor 1. Cell Growth Differ *12*, 363-369.
80. Bouvet, M., Ellis, L.M., Nishizaki, M., Fujiwara, T., Liu, W., Bucana, C.D., Fang, B., Lee, J.J., and Roth, J.A. (1998). Adenovirus-mediated wild-type p53 gene transfer down-regulates vascular endothelial growth factor expression and inhibits angiogenesis in human colon cancer. Cancer Res *58*, 2288-2292.
81. Richard, S., Campello, C., Taillandier, L., Parker, F., and Resche, F. (1998). Haemangioblastoma of the central nervous system in von Hippel-Lindau disease. French VHL Study Group. J Intern Med *243*, 547-553.
82. Sufan, R.I., Jewett, M.A., and Ohh, M. (2004). The role of von Hippel-Lindau tumor suppressor protein and hypoxia in renal clear cell carcinoma. Am J Physiol Renal Physiol *287*, F1-6.
83. Escuin, D., Simons, J.W., and Giannakakou, P. (2004). Exploitation of the HIF Axis for Cancer Therapy. Cancer Biol Ther *3*, ahead of print.
84. Rapisarda, A., Uranchimeg, B., Scudiero, D.A., Selby, M., Sausville, E.A., Shoemaker, R.H., and Melillo, G. (2002). Identification of small molecule inhibitors of hypoxia-inducible factor 1 transcriptional activation pathway. Cancer Res *62*, 4316-4324.
85. Gradin, K., McGuire, J., Wenger, R.H., Kvietikova, I., fhitelaw, M.L., Toftgard, R., Tora, L., Gassmann, M., and Poellinger, L. (1996). Functional interference between hypoxia and dioxin signal transduction pathways: competition for recruitment of the Arnt transcription factor. Mol Cell Biol *16*, 5221-5231.
86. Minet, E., Mottet, D., Michel, G., Roland, I., Raes, M., Remacle, J., and Michiels, C. (1999). Hypoxia-induced activation of HIF-1: role of HIF-1alpha-Hsp90 interaction. FEBS Lett *460*, 251-256.
87. Isaacs, J.S., Jung, Y.J., Mimnaugh, E.G., Martinez, A., Cuttitta, F., and Neckers, L.M. (2002). Hsp90 regulates a von Hippel Lindau-independent hypoxia-inducible factor-1 alpha-degradative pathway. J Biol Chem *277*, 29936-29944.

88. Mabjeesh, N.J., Post, D.E., Willard, M.T., Kaur, B., Van Meir, E.G., Simons, J.W., and Zhong, H. (2002). Geldanamycin induces degradation of hypoxia-inducible factor 1alpha protein via the proteosome pathway in prostate cancer cells. Cancer Res *62*, 2478-2482.
89. Chun, Y.S., Yeo, E.J., Choi, E., Teng, C.M., Bae, J.M., Kim, M.S., and Park, J.W. (2001). Inhibitory effect of YC-1 on the hypoxic induction of erythropoietin and vascular endothelial growth factor in Hep3B cells. Biochem Pharmacol *61*, 947-954.
90. Hsu, H.K., Juan, S.H., Ho, P.Y., Liang, Y.C., Lin, C.H., Teng, C.M., and Lee, W.S. (2003). YC-1 inhibits proliferation of human vascular endothelial cells through a cyclic GMP-independent pathway. Biochem Pharmacol *66*, 263-271.
91. Yeo, E.J., Chun, Y.S., Cho, Y.S., Kim, J., Lee, J.C., Kim, M.S., and Park, J.W. (2003). YC-1: a potential anticancer drug targeting hypoxia-inducible factor 1. J Natl Cancer Inst *95*, 516-525.
92. Jones, M.K., Szabo, I.L., Kawanaka, H., Husain, S.S., and Tarnawski, A.S. (2002). von Hippel Lindau tumor suppressor and HIF-1alpha: new targets of NSAIDs inhibition of hypoxia-induced angiogenesis. Faseb J *16*, 264-266.
93. Palayoor, S.T., Tofilon, P.J., and Coleman, C.N. (2003). Ibuprofen-mediated reduction of hypoxia-inducible factors HIF-1alpha and HIF-2alpha in prostate cancer cells. Clin Cancer Res *9*, 3150-3157.
94. Greco, O., Marples, B., Joiner, M.C., and Scott, S.D. (2003). How to overcome (and exploit) tumor hypoxia for targeted gene therapy. J Cell Physiol *197*, 312-325.
95. Fulci, G., and Chiocca, E.A. (2003). Oncolytic viruses for the therapy of brain tumors and other solid malignancies: a review. Front Biosci *8*, e346-360.
96. Post, D.E., and Van Meir, E.G. (2003). A novel hypoxia-inducible factor (HIF) activated oncolytic adenovirus for cancer therapy. Oncogene *22*, 2065-2072.
97. Sun, X., Kanwar, J.R., Leung, E., Lehnert, K., Wang, D., and Krissansen, G.W. (2001). Gene transfer of antisense hypoxia inducible factor-1 alpha enhances the therapeutic efficacy of cancer immunotherapy. Gene Ther *8*, 638-645.
98. Luduena, R.F. (1998). Multiple forms of tubulin: different gene products and covalent modifications. Int Rev Cytol *178*, 207-275.
99. Orr, G.A., Verdier-Pinard, P., McDaid, H., and Horwitz, S.B. (2003). Mechanisms of Taxol resistance related to microtubules. Oncogene *22*, 7280-7295.
100. Nicoletti, M.I., Valoti, G., Giannakakou, P., Zhan, Z., Kim, J.H., Lucchini, V., Landoni, F., Mayo, J.G., Giavazzi, R., and Fojo, T. (2001). Expression of beta-tubulin isotypes in human ovarian carcinoma xenografts and in a sub-panel of human cancer cell lines from the NCI-Anticancer Drug Screen: correlation with sensitivity to microtubule active agents. Clin Cancer Res *7*, 2912-2922.
101. Dutcher, S.K., and Trabuco, E.C. (1998). The UNI3 gene is required for assembly of basal bodies of Chlamydomonas and encodes delta-tubulin, a new member of the tubulin superfamily. Mol Biol Cell *9*, 1293-1308.
102. Vaughan, S., Attwood, T., Navarro, M., Scott, V., McKean, P., and Gull, K. (2000). New tubulins in protozoal parasites. Curr Biol *10*, R258-259.
103. Dutcher, S.K. (2001). The tubulin fraternity: alpha to eta. Curr Opin Cell Biol *13*, 49-54.
104. Oakley, B.R. (2000). An abundance of tubulins. Trends Cell Biol *10*, 537-542.
105. Oakley, C.E., and Oakley, B.R. (1989). Identification of gamma-tubulin, a new member of the tubulin superfamily encoded by mipA gene of Aspergillus nidulans. Nature *338*, 662-664.

106. Westermann, S., and Weber, K. (2003). Post-translational modifications regulate microtubule function. Nat Rev Mol Cell Biol *4*, 938-947.
107. Wittmann, T., Hyman, A., and Desai, A. (2001). The spindle: a dynamic assembly of microtubules and motors. Nat Cell Biol *3*, E28-34.
108. Gundersen, G.G., and Cook, T.A. (1999). Microtubules and signal transduction. Curr Opin Cell Biol *11*, 81-94.
109. Mallik, R., Carter, B.C., Lex, S.A., King, S.J., and Gross, S.P. (2004). Cytoplasmic dynein functions as a gear in response to load. Nature *427*, 649-652.
110. Goodson, H.V., Skube, S.B., Stalder, R., Valetti, C., Kreis, T.E., Morrison, E.E., and Schroer, T.A. (2003). CLIP-170 interacts with dynactin complex and the APC-binding protein EB1 by different mechanisms. Cell Motil Cytoskeleton *55*, 156-173.
111. Valetti, C., Wetzel, D.M., Schrader, M., Hasbani, M.J., Gill, S.R., Kreis, T.E., and Schroer, T.A. (1999). Role of dynactin in endocytic traffic: effects of dynamitin overexpression and colocalization with CLIP-170. Mol Biol Cell *10*, 4107-4120.
112. Suomalainen, M., Nakano, M.Y., Keller, S., Boucke, K., Stidwill, R.P., and Greber, U.F. (1999). Microtubule-dependent plus- and minus end-directed motilities are competing processes for nuclear targeting of adenovirus. J Cell Biol *144*, 657-672.
113. Eckley, D.M., Gill, S.R., Melkonian, K.A., Bingham, J.B., Goodson, H.V., Heuser, J.E., and Schroer, T.A. (1999). Analysis of dynactin subcomplexes reveals a novel actin-related protein associated with the arp1 minifilament pointed end. J Cell Biol *147*, 307-320.
114. Quintyne, N.J., Gill, S.R., Eckley, D.M., Crego, C.L., Compton, D.A., and Schroer, T.A. (1999). Dynactin is required for microtubule anchoring at centrosomes. J Cell Biol *147*, 321-334.
115. Goodson, H.V., Valetti, C., and Kreis, T.E. (1997). Motors and membrane traffic. Curr Opin Cell Biol *9*, 18-28.
116. Kikkawa, M., Sablin, E.P., Okada, Y., Yajima, H., Fletterick, R.J., and Hirokawa, N. (2001). Switch-based mechanism of kinesin motors. Nature *411*, 439-445.
117. Heggeness, M.H., Simon, M., and Singer, S.J. (1978). Association of mitochondria with microtubules in cultured cells. Proc Natl Acad Sci U S A *75*, 3863-3866.
118. Nangaku, M., Sato-Yoshitake, R., Okada, Y., Noda, Y., Takemura, R., Yamazaki, H., and Hirokawa, N. (1994). KIF1B, a novel microtubule plus end-directed monomeric motor protein for transport of mitochondria. Cell *79*, 1209-1220.
119. Tanaka, Y., Kanai, Y., Okada, Y., Nonaka, S., Takeda, S., Harada, A., and Hirokawa, N. (1998). Targeted disruption of mouse conventional kinesin heavy chain, kif5B, results in abnormal perinuclear clustering of mitochondria. Cell *93*, 1147-1158.
120. Terasaki, M., and Reese, T.S. (1994). Interactions among endoplasmic reticulum, microtubules, and retrograde movements of the cell surface. Cell Motil Cytoskeleton *29*, 291-300.
121. Thyberg, J., and Moskalewski, S. (1985). Microtubules and the organization of the Golgi complex. Exp Cell Res *159*, 1-16.
122. Wiemer, E.A., Wenzel, T., Deerinck, T.J., Ellisman, M.H., and Subramani, S. (1997). Visualization of the peroxisomal compartment in living mammalian cells: dynamic behavior and association with microtubules. J Cell Biol *136*, 71-80.

123. Collot, M., Louvard, D., and Singer, S.J. (1984). Lysosomes are associated with microtubules and not with intermediate filaments in cultured fibroblasts. Proc Natl Acad Sci U S A *81*, 788-792.
124. Ebneth, A., Godemann, R., Stamer, K., Illenberger, S., Trinczek, B., and Mandelkow, E. (1998). Overexpression of tau protein inhibits kinesin-dependent trafficking of vesicles, mitochondria, and endoplasmic reticulum: implications for Alzheimer's disease. J Cell Biol *143*, 777-794.
125. Gurland, G., and Gundersen, G.G. (1995). Stable, detyrosinated microtubules function to localize vimentin intermediate filaments in fibroblasts. J Cell Biol *131*, 1275-1290.
126. Jordan, M.A., and Wilson, L. (1998). Microtubules and actin filaments: dynamic targets for cancer chemotherapy. Curr Opin Cell Biol *10*, 123-130.
127. Giannakakou, P., Sackett, D.L., Ward, Y., Webster, K.R., Blagosklonny, M.V., and Fojo, T. (2000). p53 is associated with cellular microtubules and is transported to the nucleus by dynein. Nat Cell Biol *2*, 709-717.
128. Galigniana, M.D., Harrell, J.M., O'Hagen, H.M., Ljungman, M., and Pratt, W.B. (2004). Hsp90-binding immunophilins link p53 to dynein during p53 transport to the nucleus. J Biol Chem *279*, 22483-22489.
129. Hergovich, A., Lisztwan, J., Barry, R., Ballschmieter, P., and Krek, W. (2003). Regulation of microtubule stability by the von Hippel-Lindau tumour suppressor protein pVHL. Nat Cell Biol *5*, 64-70.
130. Dallol, A., Agathanggelou, A., Fenton, S.L., Ahmed-Choudhury, J., Hesson, L., Vos, M.D., Clark, G.J., Downward, J., Maher, E.R., and Latif, F. (2004). RASSF1A interacts with microtubule-associated proteins and modulates microtubule dynamics. Cancer Res *64*, 4112-4116.
131. Bearer, E.L., and Satpute-Krishnan, P. (2002). The role of the cytoskeleton in the life cycle of viruses and intracellular bacteria: tracks, motors, and polymerization machines. Curr Drug Targets Infect Disord *2*, 247-264.
132. Jansen, R.P. (2001). mRNA localization: message on the move. Nat Rev Mol Cell Biol *2*, 247-256.
133. Nagata, K., Puls, A., Futter, C., Aspenstrom, P., Schaefer, E., Nakata, T., Hirokawa, N., and Hall, A. (1998). The MAP kinase kinase kinase MLK2 co-localizes with activated JNK along microtubules and associates with kinesin superfamily motor KIF3. Embo J *17*, 149-158.
134. Thorpe, C.J., Schlesinger, A., and Bowerman, B. (2000). Wnt signalling in Caenorhabditis elegans: regulating repressors and polarizing the cytoskeleton. Trends Cell Biol *10*, 10-17.
135. Quasthoff, S., and Hartung, H.P. (2002). Chemotherapy-induced peripheral neuropathy. J Neurol *249*, 9-17.
136. Rowinsky, E.K. (1997). The development and clinical utility of the taxane class of antimicrotubule chemotherapy agents. Annu Rev Med *48*, 353-374.
137. Goa, K.L., and Faulds, D. (1994). Vinorelbine. A review of its pharmacological properties and clinical use in cancer chemotherapy. Drugs Aging *5*, 200-234.
138. Downing, K.H. (2000). Structural basis for the interaction of tubulin with proteins and drugs that affect microtubule dynamics. Annu Rev Cell Dev Biol *16*, 89-111.
139. Duflos, A., Kruczynski, A., and Barret, J.M. (2002). Novel aspects of natural and modified vinca alkaloids. Curr Med Chem Anti-Canc Agents *2*, 55-70.

140. Schiff, P.B., Fant, J., and Horwitz, S.B. (1979). Promotion of microtubule assembly in vitro by taxol. Nature *277*, 665-667.
141. Hung, D.T., Chen, J., and Schreiber, S.L. (1996). (+)-Discodermolide binds to microtubules in stoichiometric ratio to tubulin dimers, blocks taxol binding and results in mitotic arrest. Chem Biol *3*, 287-293.
142. Bollag, D.M., McQueney, P.A., Zhu, J., Hensens, O., Koupal, L., Liesch, J., Goetz, M., Lazarides, E., and Woods, C.M. (1995). Epothilones, a new class of microtubule-stabilizing agents with a taxol-like mechanism of action. Cancer Res *55*, 2325-2333.
143. Long, B.H., Carboni, J.M., Wasserman, A.J., Cornell, L.A., Casazza, A.M., Jensen, P.R., Lindel, T., Fenical, W., and Fairchild, C.R. (1998). Eleutherobin, a novel cytotoxic agent that induces tubulin polymerization, is similar to paclitaxel (Taxol). Cancer Res *58*, 1111-1115.
144. Nicolaou, K.C., Pfefferkorn, J., Xu, J., Winssinger, N., Ohshima, T., Kim, S., Hosokawa, S., Vourloumis, D., van Delft, F., and Li, T. (1999). Total synthesis and chemical biology of the sarcodictyins. Chem Pharm Bull (Tokyo) *47*, 1199-1213.
145. Mooberry, S.L., Tien, G., Hernandez, A.H., Plubrukarn, A., and Davidson, B.S. (1999). Laulimalide and isolaulimalide, new paclitaxel-like microtubule-stabilizing agents. Cancer Res *59*, 653-660.
146. Jimenez-Barbero, J., Amat-Guerri, F., and Snyder, J.P. (2002). The solid state, solution and tubulin-bound conformations of agents that promote microtubule stabilization. Curr Med Chem Anti-Canc Agents *2*, 91-122.
147. Weisenberg, R.C., Borisy, G.G., and Taylor, E.W. (1968). The colchicine-binding protein of mammalian brain and its relation to microtubules. Biochemistry *7*, 4466-4479.
148. Borisy, G.G., and Taylor, E.W. (1967). The mechanism of action of colchicine. Binding of colchincine-3H to cellular protein. J Cell Biol *34*, 525-533.
149. Hamel, E., and Lin, C.M. (1983). Interactions of combretastatin, a new plant-derived antimitotic agent, with tubulin. Biochem Pharmacol *32*, 3864-3867.
150. Cirla, A., and Mann, J. (2003). Combretastatins: from natural products to drug discovery. Nat Prod Rep *20*, 558-564.
151. Fotsis, T., Zhang, Y., Pepper, M.S., Adlercreutz, H., Montesano, R., Nawroth, P.P., and Schweigerer, L. (1994). The endogenous oestrogen metabolite 2-methoxyoestradiol inhibits angiogenesis and suppresses tumour growth. Nature *368*, 237-239.
152. Wassberg, E. (1999). Angiostatic treatment of neuroblastoma. Ups J Med Sci *104*, 1-24.
153. Sweeney, C.J., Miller, K.D., Sissons, S.E., Nozaki, S., Heilman, D.K., Shen, J., and Sledge, G.W., Jr. (2001). The antiangiogenic property of docetaxel is synergistic with a recombinant humanized monoclonal antibody against vascular endothelial growth factor or 2-methoxyestradiol but antagonized by endothelial growth factors. Cancer Res *61*, 3369-3372.
154. Kinuya, S., Kawashima, A., Yokoyama, K., Kudo, M., Kasahara, Y., Watanabe, N., Shuke, N., Bunko, H., Michigishi, T., and Tonami, N. (2001). Anti-angiogenic therapy and radioimmunotherapy in colon cancer xenografts. Eur J Nucl Med *28*, 1306-1312.
155. Huober, J.B., Nakamura, S., Meyn, R., Roth, J.A., and Mukhopadhyay, T. (2000). Oral administration of an estrogen metabolite-induced potentiation of radiation antitumor effects in presence of wild-type p53 in non-small- cell lung cancer. Int J Radiat Oncol Biol Phys *48*, 1127-1137.

156. Klauber, N., Parangi, S., Flynn, E., Hamel, E., and D'Amato, R.J. (1997). Inhibition of angiogenesis and breast cancer in mice by the microtubule inhibitors 2-methoxyestradiol and taxol. Cancer Res *57*, 81-86.
157. Josefsson, E., and Tarkowski, A. (1997). Suppression of type II collagen-induced arthritis by the endogenous estrogen metabolite 2-methoxyestradiol. Arthritis Rheum *40*, 154-163.
158. Liehr, J.G., Fang, W.F., Sirbasku, D.A., and Ari-Ulubelen, A. (1986). Carcinogenicity of catechol estrogens in Syrian hamsters. J Steroid Biochem *24*, 353-356.
159. Rajan, R., Reddy, V.V., Reichle, F., David, J.S., and Daly, M.J. (1984). Effects of catechol estrogen methyl ethers on lipid metabolism in prepubertal rats. Steroids *43*, 499-507.
160. Yue, T.L., Wang, X., Louden, C.S., Gupta, S., Pillarisetti, K., Gu, J.L., Hart, T.K., Lysko, P.G., and Feuerstein, G.Z. (1997). 2-Methoxyestradiol, an endogenous estrogen metabolite, induces apoptosis in endothelial cells and inhibits angiogenesis: possible role for stress-activated protein kinase signaling pathway and Fas expression. Mol Pharmacol *51*, 951-962.
161. Chauhan, D., Li, G., Hideshima, T., Podar, K., Mitsiades, C., Mitsiades, N., Munshi, N., Kharbanda, S., and Anderson, K.C. (2003). JNK-dependent release of mitochondrial protein, Smac, during apoptosis in multiple myeloma (MM) cells. J Biol Chem *278*, 17593-17596.
162. LaVallee, T.M., Zhan, X.H., Johnson, M.S., Herbstritt, C.J., Swartz, G., Williams, M.S., Hembrough, W.A., Green, S.J., and Pribluda, V.S. (2003). 2-methoxyestradiol up-regulates death receptor 5 and induces apoptosis through activation of the extrinsic pathway. Cancer Res *63*, 468-475.
163. LaVallee, T.M., Zhan, X.H., Herbstritt, C.J., Kough, E.C., Green, S.J., and Pribluda, V.S. (2002). 2-Methoxyestradiol Inhibits Proliferation and Induces Apoptosis Independently of Estrogen Receptors alpha and beta. Cancer Res *62*, 3691-3697.
164. Klauber, N., Parangi, S., Flynn, E., Hamel, E., and D'Amato, R.J. (1997). Inhibition of angiogenesis and breast cancer in mice by the microtubule inhibitors 2-methoxyestradiol and taxol. Cancer Res *57*, 81-86.
165. Qadan, L.R., Perez-Stable, C.M., Anderson, C., D'Ippolito, G., Herron, A., Howard, G.A., and Roos, B.A. (2001). 2-Methoxyestradiol induces G2/M arrest and apoptosis in prostate cancer. Biochem Biophys Res Commun *285*, 1259-1266.
166. D'Amato, R.J., Lin, C.M., Flynn, E., Folkman, J., and Hamel, E. (1994). 2-Methoxyestradiol, an endogenous mammalian metabolite, inhibits tubulin polymerization by interacting at the colchicine site. Proc Natl Acad Sci U S A *91*, 3964-3968.
167. Cushman, M., He, H.M., Katzenellenbogen, J.A., Lin, C.M., and Hamel, E. (1995). Synthesis, antitubulin and antimitotic activity, and cytotoxicity of analogs of 2-methoxyestradiol, an endogenous mammalian metabolite of estradiol that inhibits tubulin polymerization by binding to the colchicine binding site. J Med Chem *38*, 2041-2049.
168. Verdier-Pinard, P., Wang, Z., Mohanakrishnan, A.K., Cushman, M., and Hamel, E. (2000). A steroid derivative with paclitaxel-like effects on tubulin polymerization. Mol Pharmacol *57*, 568-575.
169. Hamel, E., Lin, C.M., Flynn, E., and D'Amato, R.J. (1996). Interactions of 2-methoxyestradiol, an endogenous mammalian metabolite, with unpolymerized tubulin and with tubulin polymers. Biochemistry *35*, 1304-1310.

170. Aizu-Yokota, E., Susaki, A., and Sato, Y. (1995). Natural estrogens induce modulation of microtubules in Chinese hamster V79 cells in culture. Cancer Res *55*, 1863-1868.
171. Lottering, M.L., de Kock, M., Viljoen, T.C., Grobler, C.J., and Seegers, J.C. (1996). 17beta-Estradiol metabolites affect some regulators of the MCF-7 cell cycle. Cancer Lett *110*, 181-186.
172. Attalla, H., Makela, T.P., Adlercreutz, H., and Andersson, L.C. (1996). 2-Methoxyestradiol arrests cells in mitosis without depolymerizing tubulin. Biochem Biophys Res Commun *228*, 467-473.
173. Hlatky, L., Hahnfeldt, P., and Folkman, J. (2002). Clinical application of antiangiogenic therapy: microvessel density, what it does and doesn't tell us. J Natl Cancer Inst *94*, 883-893.
174. Weidner, N., Semple, J.P., Welch, W.R., and Folkman, J. (1991). Tumor angiogenesis and metastasis--correlation in invasive breast carcinoma. N Engl J Med *324*, 1-8.
175. Hamel, E., Lin, C.M., Plowman, J., Wang, H.K., Lee, K.H., and Paull, K.D. (1996). Antitumor 2,3-dihydro-2-(aryl)-4(1H)-quinazolinone derivatives. Interactions with tubulin. Biochem Pharmacol *51*, 53-59.
176. Hamel, E. (1992). Natural products which interact with tubulin in the vinca domain: maytansine, rhizoxin, phomopsin A, dolastatins 10 and 15 and halichondrin B. Pharmacol Ther *55*, 31-51.
177. Semenza, G.L. (2000). HIF-1: mediator of physiological and pathophysiological responses to hypoxia. J Appl Physiol *88*, 1474-1480.
178. Wenger, R.H. (2000). Mammalian oxygen sensing, signalling and gene regulation. J Exp Biol *203 Pt 8*, 1253-1263.
179. Post, D.E., and Van Meir, E.G. (2001). Generation of bidirectional hypoxia/HIF-responsive expression vectors to target gene expression to hypoxic cells. Gene Ther. *8*, 1801-1807.
180. Mabjeesh, N.J., Post, D.E., Willard, M.T., Kaur, B., Van Meir, E.G., Simons, J.W., and Zhong, H. (2002). Geldanamycin induces degradation of hypoxia-inducible factor 1alpha protein via the proteosome pathway in prostate cancer cells. Cancer Res *62*, 2478-2482.
181. Isaacs, J.S., Jung, Y.J., Mimnaugh, E.G., Martinez, A., Cuttitta, F., and Neckers, L.M. (2002). Hsp90 Regulates a von Hippel Lindau-independent Hypoxia-inducible Factor-1alpha -degradative Pathway. J Biol Chem *277*, 29936-29944.
182. Purohit, A., Singh, A., Ghilchik, M.W., and Reed, M.J. (1999). Inhibition of tumor necrosis factor alpha-stimulated aromatase activity by microtubule-stabilizing agents, paclitaxel and 2-methoxyestradiol. Biochem Biophys Res Commun *261*, 214-217.
183. Mayer, T.U., Kapoor, T.M., Haggarty, S.J., King, R.W., Schreiber, S.L., and Mitchison, T.J. (1999). Small molecule inhibitor of mitotic spindle bipolarity identified in a phenotype-based screen. Science *286*, 971-974.
184. Gagescu, R. (2000). Another star on drugs. Nat Rev Mol Cell Biol *1*, 5.
185. Giannakakou, P., Sackett, D.L., Kang, Y.K., Zhan, Z., Buters, J.T., Fojo, T., and Poruchynsky, M.S. (1997). Paclitaxel-resistant human ovarian cancer cells have mutant beta- tubulins that exhibit impaired paclitaxel-driven polymerization. J Biol Chem *272*, 17118-17125.
186. Cushman, M., He, H.M., Katzenellenbogen, J.A., Varma, R.K., Hamel, E., Lin, C.M., Ram, S., and Sachdeva, Y.P. (1997). Synthesis of analogs of 2-methoxyestradiol with

enhanced inhibitory effects on tubulin polymerization and cancer cell growth. J Med Chem *40*, 2323-2334.

187. Seegers, J.C., Lottering, M.L., Grobler, C.J., van Papendorp, D.H., Habbersett, R.C., Shou, Y., and Lehnert, B.E. (1997). The mammalian metabolite, 2-methoxyestradiol, affects P53 levels and apoptosis induction in transformed cells but not in normal cells. J Steroid Biochem Mol Biol *62*, 253-267.
188. Dark, G.G., Hill, S.A., Prise, V.E., Tozer, G.M., Pettit, G.R., and Chaplin, D.J. (1997). Combretastatin A-4, an agent that displays potent and selective toxicity toward tumor vasculature. Cancer Res *57*, 1829-1834.
189. Tozer, G.M., Prise, V.E., Wilson, J., Cemazar, M., Shan, S., Dewhirst, M.W., Barber, P.R., Vojnovic, B., and Chaplin, D.J. (2001). Mechanisms associated with tumor vascular shut-down induced by combretastatin A-4 phosphate: intravital microscopy and measurement of vascular permeability. Cancer Res *61*, 6413-6422.
190. Grosios, K., Holwell, S.E., McGown, A.T., Pettit, G.R., and Bibby, M.C. (1999). In vivo and in vitro evaluation of combretastatin A-4 and its sodium phosphate prodrug. Br J Cancer *81*, 1318-1327.
191. Blakey, D.C., Westwood, F.R., Walker, M., Hughes, G.D., Davis, P.D., Ashton, S.E., and Ryan, A.J. (2002). Antitumor Activity of the Novel Vascular Targeting Agent ZD6126 in a Panel of Tumor Models. Clin Cancer Res *8*, 1974-1983.
192. Belotti, D., Vergani, V., Drudis, T., Borsotti, P., Pitelli, M.R., Viale, G., Giavazzi, R., and Taraboletti, G. (1996). The microtubule-affecting drug paclitaxel has antiangiogenic activity. Clin Cancer Res *2*, 1843-1849.
193. Sweeney, C.J., Miller, K.D., Sissons, S.E., Nozaki, S., Heilman, D.K., Shen, J., and Sledge, G.W., Jr. (2001). The antiangiogenic property of docetaxel is synergistic with a recombinant humanized monoclonal antibody against vascular endothelial growth factor or 2-methoxyestradiol but antagonized by endothelial growth factors. Cancer Res *61*, 3369-3372.
194. Taraboletti, G., Micheletti, G., Rieppi, M., Poli, M., Turatto, M., Rossi, C., Borsotti, P., Roccabianca, P., Scanziani, E., Nicoletti, M.I., Bombardelli, E., Morazzoni, P., Riva, A., and Giavazzi, R. (2002). Antiangiogenic and antitumor activity of IDN 5390, a new taxane derivative. Clin Cancer Res *8*, 1182-1188.
195. Chauhan, D., Catley, L., Hideshima, T., Li, G., Leblanc, R., Gupta, D., Sattler, M., Richardson, P., Schlossman, R.L., Podar, K., Weller, E., Munshi, N., and Anderson, K.C. (2002). 2-Methoxyestradiol overcomes drug resistance in multiple myeloma cells. Blood *100*, 2187-2194.
196. Banerjeei, S.K., Zoubine, M.N., Sarkar, D.K., Weston, A.P., Shah, J.H., and Campbell, D.R. (2000). 2-Methoxyestradiol blocks estrogen-induced rat pituitary tumor growth and tumor angiogenesis: possible role of vascular endothelial growth factor. Anticancer Res *20*, 2641-2645.
197. Ratcliffe, P.J. (2003). New insights into an enigmatic tumour suppressor. Nat Cell Biol *5*, 7-8.
198. Lakhani, N.J., Sarkar, M.A., Venitz, J., and Figg, W.D. (2003). 2-Methoxyestradiol, a promising anticancer agent. Pharmacotherapy *23*, 165-172.
199. Jiang, B.H., Semenza, G.L., Bauer, C., and Marti, H.H. (1996). Hypoxia-inducible factor 1 levels vary exponentially over a physiologically relevant range of O2 tension. Am. J. Physiol. *271*, C1172-1180.

200. Hale, I.L., and Matsumoto, B. (1993). Resolution of subcellular detail in thick tissue sections: immunohistochemical preparation and fluorescence confocal microscopy. Methods Cell Biol *38*, 289-324.
201. Kvietikova, I., Wenger, R.H., Marti, H.H., and Gassmann, M. (1995). The transcription factors ATF-1 and CREB-1 bind constitutively to the hypoxia-inducible factor-1 (HIF-1) DNA recognition site. Nucleic Acids Res *23*, 4542-4550.